

## 11. SITE 640<sup>1</sup>

### Shipboard Scientific Party<sup>2</sup>

#### HOLE 640A

Date occupied: 4 June 1985

Date departed: 6 June 1985

Time on hole: 2 day, 1 hr

Position: 42°00.7'N, 12°27.8'W

Water depth (sea level, corrected m, echo-sounding): 5196

Water depth (rig floor, corrected m, echo-sounding): 5206

Bottom felt (m, drill pipe): 5201

Penetration (m): 232.2

Number of cores: 9

Total length of cored section (m): 86.8

Total core recovered (m): 15.6

Core recovery (%): 18

#### Deepest sedimentary unit cored:

Depth sub-bottom (m): 232.2

Nature: sandstone

Age: Hauterivian

**Principal results:** Site 640 is on a buried ridge where Neogene turbidites overlie a thick (about 2 s), acoustically incoherent unit that rests on a strong, laterally extensive reflector thought by many workers to represent the boundary between ductile and brittle crust, in which listric faults merge at depth. The main results of drilling at Site 640 are summarized in Figure 1.

The sedimentary section comprises three lithologic units:

Lithologic Unit I, 145–157 m: Brown clay composed almost entirely of recrystallized clay minerals. Aside from fish teeth and rare agglutinated benthic foraminifers, this unit is barren of microfossils and is interpreted as being pelagic sediment accumulated below the carbonate compensation depth (CCD).

Lithologic Unit II, 157–165 m: Aptian olive-gray clay and white and olive-yellow clayey ooze with abundant nannofossils. This unit is interpreted as being pelagic sediment.

Lithologic Unit III, 165–232 m: Hauterivian to Barremian interbedded marlstone and clayey ooze, including thin turbidites with plant debris, overlying Hauterivian sandy turbidites rich in mica and plant debris. The upper part of this unit is Barremian in age. This unit is interpreted as being a sequence of terrigenous turbidites grading upward into a sequence of interbedded distal terrigenous turbidites and pelagic and hemipelagic sediments.

Laboratory measurements of sound velocity in the core samples indicate that the top of the acoustically incoherent unit is correlated with the top of the Hauterivian turbidites.

Finding Lower Cretaceous, syn-rift turbidite sediments, similar to those at Site 638, in the acoustically incoherent unit may force reassessment of the brittle/ductile-transition interpretation of the S reflector because the rocks above the S reflector at least partly consist of Early Cretaceous sediments, more or less tilted and slumped during rifting. Thus, the S reflector, lying 2–4 km below the seafloor, could represent the substratum of the syn-rift Cretaceous sedimentary rocks, formed either by the top of the pre-rift platform carbonates or by crystalline basement.

#### BACKGROUND AND OBJECTIVES

Between the tilted block drilled at Sites 638 and 639 and the peridotite ridge drilled at Site 637, the deep margin of Galicia is about 50 km wide. The seafloor, which slopes gently to the west, from 4800 to 5300 m, is broken by only one small seamount at 42°09'N, 12°32'W, which marks the outcrop of a buried north-trending ridge bringing acoustic basement (actually a zone of incoherent reflections) close to the seafloor (Fig. 2). The two north-trending sedimentary basins flanking the ridge contain thick (2–3 km) syn- and post-rift sedimentary sequences. Clearly, the buried basin-and-range topography of the "acoustic basement" is pre-Albian and probably Early Cretaceous in age (Montadert et al., 1979; Boillot et al., 1979, 1980; Sibuet et al., this volume).

This part of the margin is characterized by a deep, strong, and almost continuous reflector within the "acoustic basement," labeled "S" by Montadert et al. (1979). The S reflector is between 1.5 and 3 s (two-way traveltime) below the seafloor and thus too deep for ODP drilling (Fig. 3). Drilling into the upper part of the acoustically incoherent interval between S and the

<sup>1</sup> Boillot, G., Winterer, E. L., Meyer, A. W., et al., *Proc. Init. Repts. (Pt. A)*, ODP, 103.

<sup>2</sup> Gilbert Boillot (Co-Chief Scientist), Laboratoire de Géodynamique Sous-Marine, Université Pierre et Marie Curie, B.P. 48, 06230, Villefranche-sur-Mer, France; Edward L. Winterer (Co-Chief Scientist), Graduate Research Division A-012-W, Scripps Institution of Oceanography, La Jolla, CA 92093; Audrey W. Meyer (ODP Staff Scientist), Ocean Drilling Program, Texas A&M University, College Station, TX 77843-3469; Joseph Applegate, Department of Geology, Florida State University, Tallahassee, FL 32306; Miriam Baltuck, Department of Geology, Tulane University, New Orleans, LA 70118 (current address: NASA Headquarters, Code EEL, Washington, D.C. 20546); James A. Bergen, Department of Geology, Florida State University, Tallahassee, FL 32306; M. C. Comas, Departamento Estratigrafía y Paleontología, Facultad de Ciencias, Universidad de Granada, 18001 Granada, Spain; Thomas A. Davies, Institute for Geophysics, University of Texas at Austin, 4920 North IH 35, Austin, TX 78751; Keith Dunham, Department of Atmospheric and Oceanic Sciences, University of Michigan, 2455 Hayward Avenue, Ann Arbor, MI 48109 (current address: P.O. Box 13, Pequot Lakes, MN 56478); Cynthia A. Evans, Department of Geology, Colgate University, Hamilton, NY 13346 (current address: Lamont-Doherty Geological Observatory, Palisades, NY 10964); Jacques Girardeau, Laboratoire de Matériaux Terrestres, I.P.G., 4 Place Jussieu, 75252 Paris Cedex 05, France; David Goldberg, Lamont-Doherty Geological Observatory, Palisades, NY 10964; Janet Haggerty, Department of Geology, University of Tulsa, 600 S. College Avenue, Tulsa, OK 74104; Lubomir F. Jansa, Atlantic Geoscience Center, Bedford Institute of Oceanography, Dartmouth, Nova Scotia B2Y 4A2, Canada; Jeffrey A. Johnson, Department of Earth and Space Sciences, University of California, Los Angeles, CA 90024 (current address: 9449 Briar Forest Drive, No. 3544, Houston, TX 77063); Junzo Kasahara, Earthquake Research Institute, University of Tokyo, 1-1-1 Yayoi, Bunkyo, Tokyo 113, Japan (current address: Nippon Schlumberger K. K. 2-1 Fuchinobe, 2-Chome, Sagami-hari-shi, Kanagawa-ken, 229, Japan); Jean-Paul Loreau, Laboratoire de Géologie, Muséum National d'Histoire Naturelle, 43 Rue Buffon, 75005 Paris, France; Emilio Luna, Hispanoil, Pz Volador No. 2, 28007 Madrid, Spain; Michel Moulade, Laboratoire de Géologie et Micropaleontologie Marines, Université de Nice, Parc Valrose, 06034 Nice Cedex, France; James Ogg, Geological Research Division A-012, Scripps Institution of Oceanography, La Jolla, CA 92093 (current address: Dept. Earth and Atmospheric Sciences, Purdue University, W. Lafayette, IN 47907); Massimo Sarti, Istituto di Geologia, Università di Ferrara, Corso Ercole d'Este, 32, 44100 Ferrara, Italy; Jürgen Thürow, Institut und Museum für Geologie und Paläontologie, Universität Tübingen, Sigwartstr. 10, D-7400 Tübingen, Federal Republic of Germany; Mark A. Williamson, Atlantic Geoscience Centre, Geological Survey of Canada, Bedford Institute of Oceanography, Box 1006, Dartmouth, Nova Scotia B2Y 4A2, Canada (current address: Shell Canada Ltd., P.O. Box 100, Stn. M, Calgary, Alberta T2P 2H5, Canada).

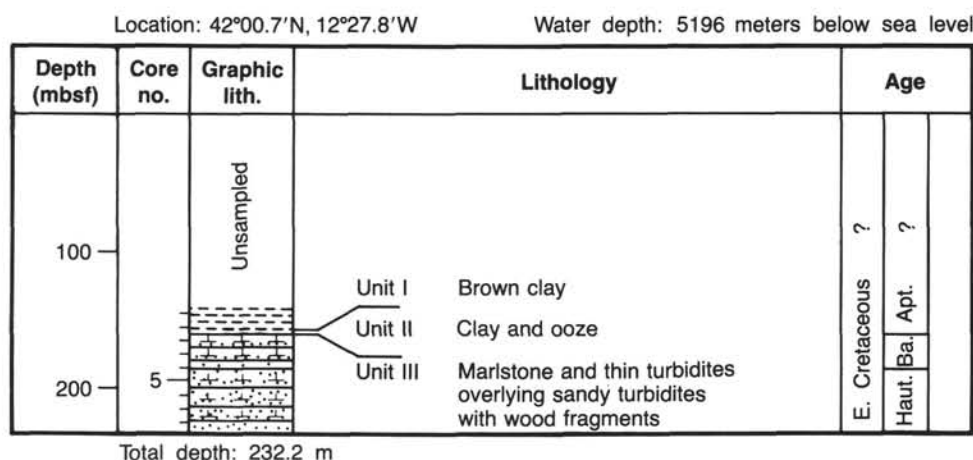


Figure 1. Stratigraphic summary log, Site 640 (Hole 640A).

prominent reflector between seismic units 3 and 4 (Fig. 3), which includes at least some syn-rift sediments (seismic unit 4), should acquire new data for interpretation of the S reflector and thus of the whole margin.

The S reflector is interpreted by Montadert et al. (1979) and Chenet et al. (1982) as being the boundary between brittle and ductile continental crust, i.e., the fault surface where listric normal faults root. This interpretation implies that the upper part of the rocks between S and the reflector at the base of seismic unit 3 consists of several tilted crustal blocks, one of which constitutes the north-trending ridge near the 12°30'W meridian (Fig. 2). According to this interpretation, the rocks above reflector S should be continental basement and/or pre-rift sediments. In this model, the margin would extend as far west as the east edge of the peridotite ridge, which is the interpretation we accept for Site 637 (see Site 637 chapter, this volume).

Before drilling at Site 640, we considered two other hypotheses as being viable:

1. The acoustically incoherent unit above the S reflector is a giant slide of pre- and syn-rift sediments, including limestone and sandstone. The S reflector would, thus, correspond to the detachment surface separating the allochthonous sedimentary cover of low acoustic impedance from the underlying autochthonous basement, which has high impedance. This hypothesis does not differentiate continental from oceanic basement beneath S.

2. The acoustically incoherent unit above the S reflector is basalt. This hypothesis results from a comparison of the deep Galicia margin with the Goban Spur margin, drilled during Deep Sea Drilling Project Leg 80 (de Graciansky, Poag, et al., 1985). Coring at Site 551, on a crustal block thought from previous studies to be a continental tilted block, recovered tholeiitic basalt. A seismic line recorded near Site 551 shows syn-rift sediments below the acoustical body identified as basalt by the drilling. This line suggests either that basalts are syn-rift volcanic deposits, resting upon thinned continental crust (Masson et al., 1985) or that early post-rift sediments derived from the continental margin are interbedded with ocean basalt. Basalts at Site 551 are similar to basalt cored at Site 550, which is clearly located on the oceanic crust. Thus, Site 551 also could belong to the oceanic domain (Maury et al., 1985).

If we should recover basalt at Site 640, the volcanics could be syn-rift extrusions or Layer 2 of a pre-Albian piece of oceanic crust. Horizon S would then perhaps be the boundary between Layers 2 and 3, and we would need to reinterpret the emplacement of the peridotite ridge at Site 637.

Drilling at Site 640 is thus crucial for the interpretation of the margin and of the adjacent oceanic basin. The major hypotheses could be tested by drilling only a few cores into the acoustically incoherent unit.

## OPERATIONS

### Approach to Site 640

For the transit from Site 639 to Site 640, a multichannel seismic line (Fig. 3) guided us, and the ship headed southwest from Site 639 to join the track of that line, following it into the chosen site near shotpoint 1765. This point is on the western summit of a ridgecrest that has two summits about 1.5 km apart. Our effort to locate the site at exactly this shotpoint was unsuccessful because, first, the satellite-navigation system does not allow the precision of navigation required to follow exactly along the multichannel line and, second, the seismic equipment on *JOIDES Resolution* (a single-channel system, digitally recorded) has an advance rate of the recording paper that produces real-time records with large vertical exaggeration, which makes it difficult to discriminate features that are close together along the profile.

The track of *JOIDES Resolution* during the approach to Site 640 is shown in Figure 4, which also shows the location of the multichannel line and key shotpoints. During the last stages of the approach, we dropped the acoustic beacon at 0100 hr on 4 June 1985, at a point about 100 m north of the multichannel line near shotpoint 1793, which is about 1.5 km east of shotpoint 1765, on the eastern summit of the buried ridge (Figure 3).

### Drilling and Coring Operations at Site 640

The objective at Site 640 was to sample the acoustically complex body underlying the post-rift sedimentary sequence. Because the seismic profiles show that the covering layers are doubtless the correlatives of the Neogene sequence cored continuously at Site 637, only about 35 km to the west, we obtained permission to wash through the soft sediments and begin coring at the top of the first sign of firm material. At 0945 hr, only about 8 hr after we had dropped the beacon, Hole 640A was spudded at a depth of 5201 m below the derrick floor. Using a center bit, we drilled ahead without coring to a depth of 145.4 mbsf, where firm material was encountered. Cores were recovered continuously from this level to the total depth of 232.2 mbsf, under normal drilling conditions. Below 157 mbsf, the section consists of Lower Cretaceous claystone and sandstone similar to the strata cored at Site 638. Recovery rates are disap-

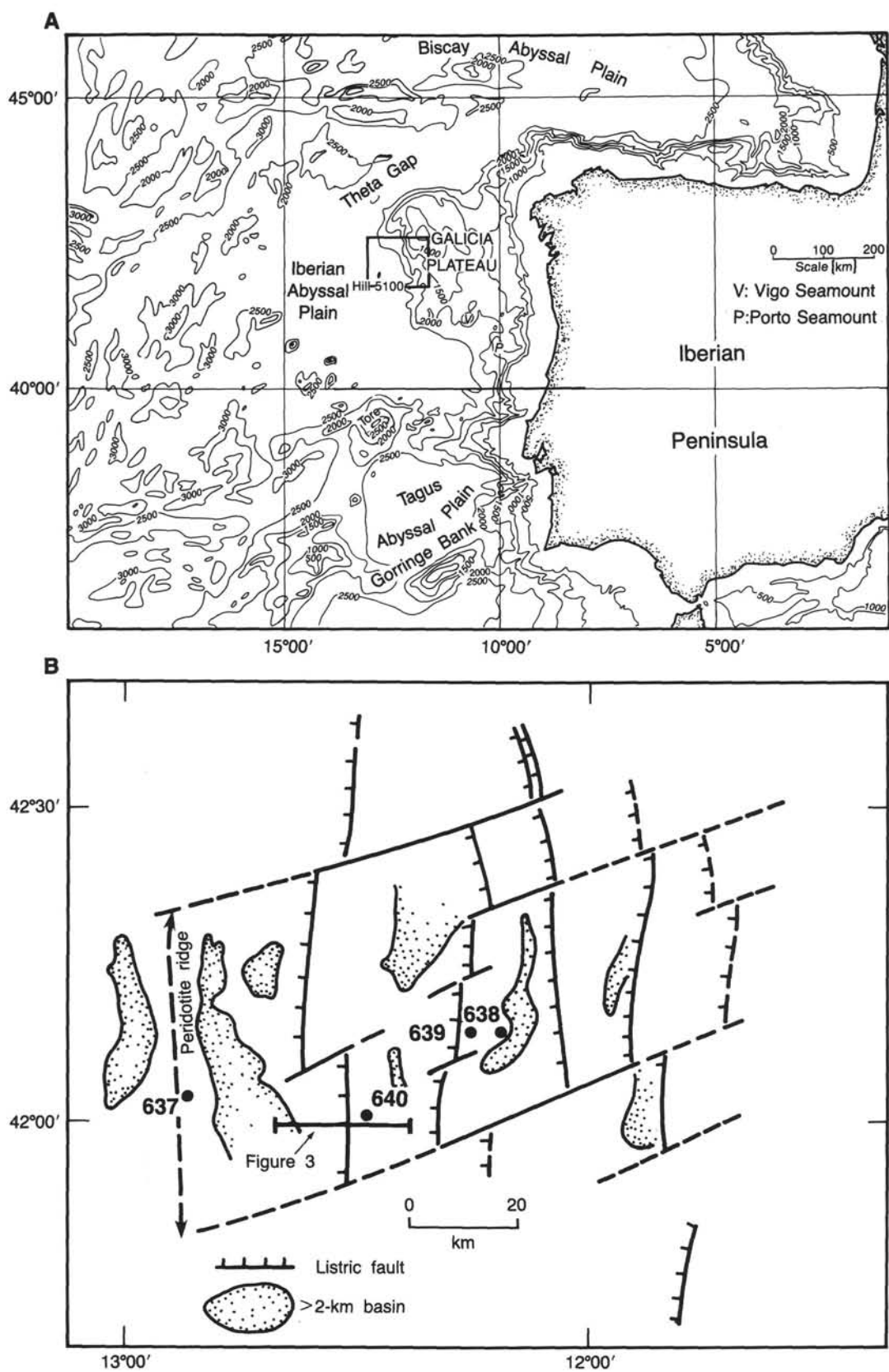


Figure 2. A. Bathymetric map of Galicia margin and surrounding area. Contour interval, 500 m. Block outlines area shown in B. B. Structural diagram of deep Galicia margin, with location of Sites 637, 638, 639, and 640 and of the seismic line shown in Figure 3.

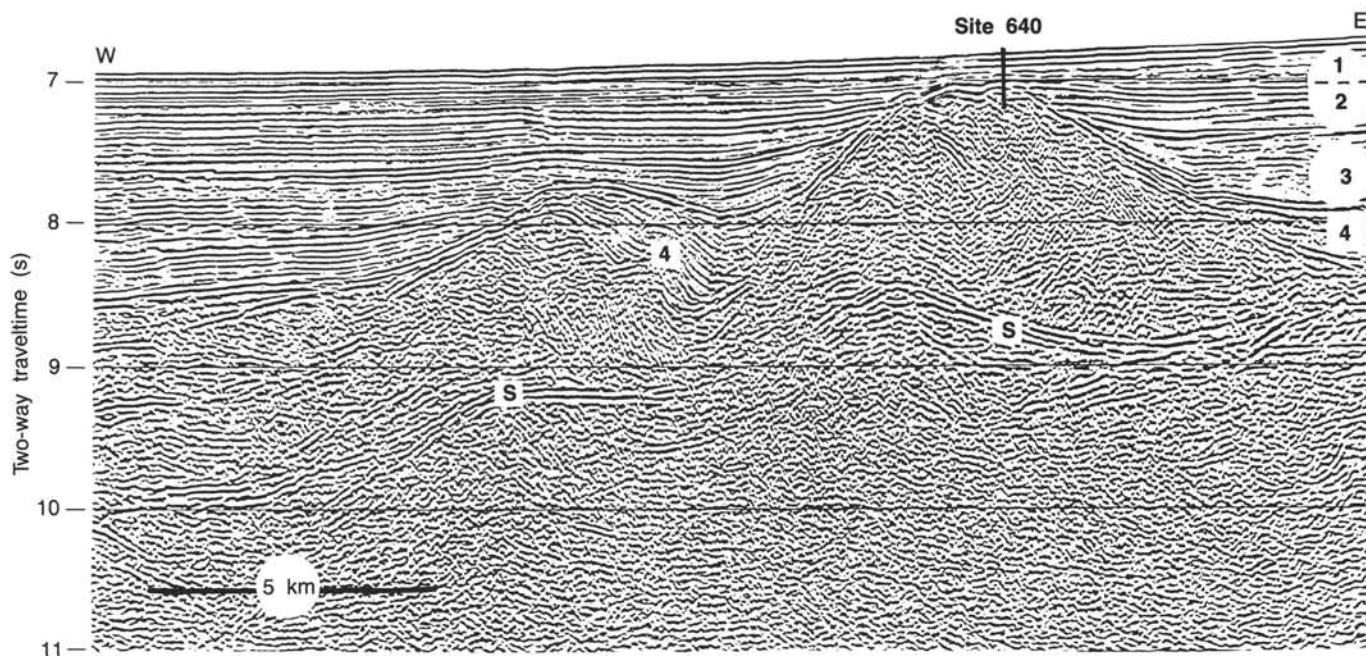


Figure 3. IFP multichannel seismic line GP-102B1, from shotpoints 1470 to 1900, showing location of Site 640 (courtesy of L. Montadert). 1-3 = Albian-Recent post-rift sediments. 4 = syn-rift sediments. S = deep reflector in "acoustical basement." Location of seismic line is shown in Figure 2.

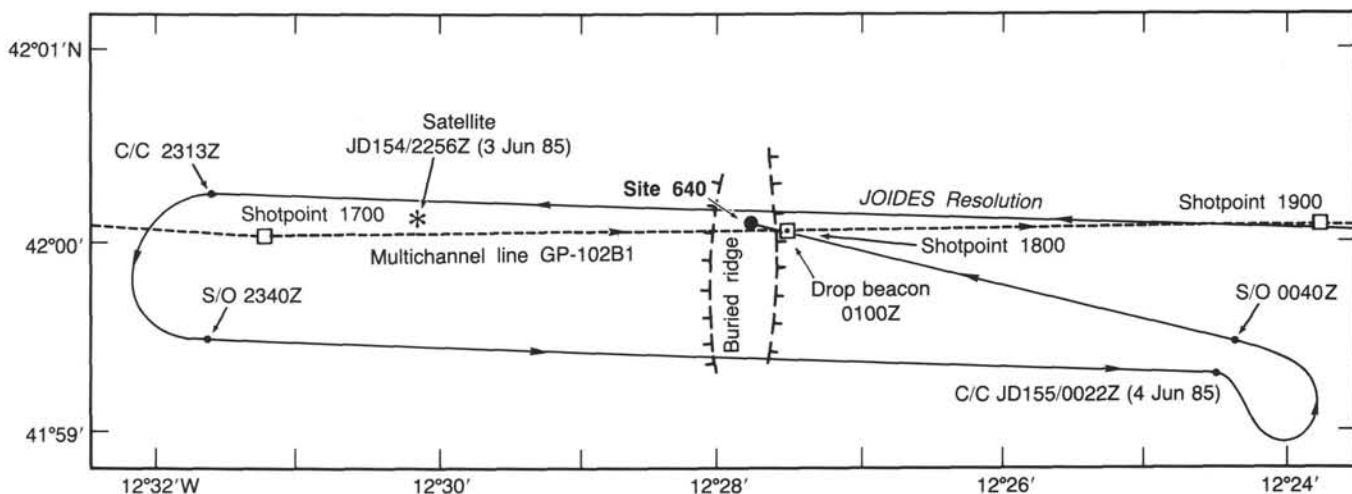


Figure 4. Track of *JOIDES Resolution* during the approach to Site 640 (solid line), showing the relation of the site to the summit area of the buried ridge. Location of multichannel line GP-102B1 (dashed line) and key shotpoints along that line are also shown.

pointingly low, averaging about 17% in the Cretaceous rocks. Table 1 gives the details on the coring record at Site 640.

We abandoned the hole because we had established that at least the upper part of the acoustically complex unit beneath the Neogene consists of Lower Cretaceous turbidite beds. We saw no pressing scientific need to continue coring deeper into a formation we had already sampled extensively at Site 638.

At 0200 hr on 6 June, about 49 hr after dropping the beacon at the site, we had pulled out of the hole and were under way back to Site 639 to complete the drilling there.

#### SEDIMENT LITHOLOGY

Drilling at Site 640 penetrated only the upper part of the sedimentary sequence. The sedimentary section sampled (Table 2) consists of brown clay (lithologic Unit I), presumed to be Late

Cretaceous or Paleogene in age, overlying a sequence of Early Cretaceous marlstone, sandstone, and limestone (lithologic Units II and III). The uppermost 145 m of section, above the brown clay, were not sampled.

#### Lithologic Unit I (145.4–156.9 m; Core 103-640A-1R through Sample 103-640A-2R-2, 32 cm)

Lithologic Unit I consists of unfossiliferous brown and yellowish brown clay, faintly mottled and with diffuse banding on a scale of 1–10 cm. Dark-gray or black spots and patches as much as 0.6 cm across rich in organic matter or iron-manganese oxide occur throughout. Smear slides show the sediment to be composed almost entirely of recrystallized clay minerals and trace amounts of quartz silt and carbonate rhombs. Fish teeth are common in washed residues of the sediments.



**Table 1. Coring summary, Site 640 (Hole 640A).**

Core no.	Date (mo./day) 1985	Time (hr)	Sub-bottom top (m)	Sub-bottom bottom (m)	Length cored (m)	Length recovered (m)	Percentage recovered
1R	06/04	1855	145.4	155.1	9.7	1.5	15.0
2R	06/04	2230	155.1	164.7	9.6	2.5	25.0
3R	06/05	0100	164.7	174.3	9.6	4.7	48.0
4R	06/05	0330	174.3	184.0	9.7	2.0	20.0
5R	06/05	0600	184.0	193.7	9.7	0.3	3.0
6R	06/05	0845	193.7	203.3	9.6	1.6	16.0
7R	06/05	1145	203.3	213.0	9.7	1.7	17.0
8R	06/05	1415	213.0	222.5	9.5	1.1	11.0
9R	06/05	1645	222.5	232.2	9.7	0.2	2.0

**Table 2. Lithologic units sampled at Site 640.**

Lithologic unit/subunit	Lithology	Cores	Sub-bottom depth (m)
I	Brown clay	103-640A-1R-1, 0 cm–103-640A-2R-2, 32 cm	145.4–156.9
II	Clayey ooze	103-640A-2R-2, 32 cm–103-640A-2R, CC	156.9–164.7
IIIA	Marlstone and clayey ooze	103-640A-3R-1, 0 cm–103-640A-5R-1, 4 cm	164.7–184.4
IIIB	Sandstone, limestone, and marlstone microturbidites	103-640A-5R-1, 4 cm–103-640A-9R, CC	184.4–232.2

The upper boundary of lithologic Unit I remains unknown because the top 145 m of the section were not cored. The bottom of lithologic Unit I is marked by an abrupt lithologic change to olive-gray clay, which forms the top of lithologic Unit II (Fig. 5). This sharp boundary probably represents a major hiatus in sedimentation, although we found no clear evidence of this.

In the absence of good biostratigraphic control, we can say with certainty only that lithologic Unit I is younger than Early Cretaceous. Comparison with other sites in the northeast Atlantic suggests a Paleogene age (see later discussion).

#### **Lithologic Unit II (156.9–164.7 m; Samples 103-640A-2R-2, 32 cm, through 103-640A-2R, CC)**

Directly beneath lithologic Unit I and extending down to the base of Sample 103-640A-2R, CC, lithologic Unit II consists of olive-gray clay and white and olive-yellow clayey ooze. The uppermost part of lithologic Unit II is a 15-cm-thick band of olive-gray clay having limonitic patches and many blue-black laminae. The sediment is barren of fossils, except some agglutinated foraminifers. Below the clay, the sediment is a clayey ooze composed of loose crystals of recrystallized carbonate having a high proportion of well-preserved nannofossils. The boundary between the clay and the clayey ooze is abrupt and may be a drilling contact or a hiatus in sedimentation. The ooze becomes increasingly yellow and more clay-rich downward. The distinct lithologic change between lithologic Unit II and lithologic Unit III suggests that the boundary between these units (which lies between Cores 103-640A-2R and 103-640A-3R) may represent a hiatus in sedimentation.

#### **Lithologic Unit III (164.7–232.2 m; Cores 103-640A-3R through 103-640A-9R)**

##### **Subunit IIIA (164.7–184.4 m; Core 103-640A-3R through Sample 103-640A-5R-1, 4 cm)**

Subunit IIIA consists of dark-gray calcareous clay and marl and white clayey ooze. Marl and clayey ooze alternate at intervals ranging from 15 to 100 cm. In some places, the dark-gray marl layers have sharp bases and gradational tops; in others,

both upper and lower boundaries are gradational. The dark-gray marl layers are finely, though faintly, laminated and contain abundant plant debris, including recognizable wood fragments, one being 5 cm long. The light-gray clayey ooze layers are massive and faintly mottled. They consist largely of recrystallized carbonate and some nannofossils, including nannocoids. Some of the clayey ooze beds include intervals from 10 to 20 cm thick that are darker and more clay-rich. The clayey ooze has been lithified to a clayey limestone in some intervals in Cores 103-640A-3R and 103-640A-4R.

Clayey ooze is interpreted as being pelagic sediment. The more clay-rich intervals and the marl beds represent intervals of increased terrigenous input, probably as both distal turbidites and increased nepheloid transport.

##### **Subunit IIIB (184.4–232.2 m; Sample 103-640A-5R-1, 4 cm, through Core 103-640A-9R)**

Subunit IIIB consists of calcareous clay, silty calcareous clay, clayey limestone, and sandstone. Because of poor core recovery, the details of the contact between Subunits IIIA and IIIB are unknown, but the contact is most likely gradational. Drilling terminated before the lower boundary of Subunit IIIB was reached.

The calcareous clay and silty calcareous clay in Subunit IIIB are interbedded on a scale of millimeters to 3 cm. Each bed is normally graded from dark-gray silty calcareous clay, rich in mica and plant debris, up into lighter gray calcareous clay. The lower part of each interval commonly shows parallel lamination. Several thin marl interbeds occur. The bedding in the clays, especially in Cores 103-640A-6R and 103-640A-7R, is highly contorted and has the appearance of slumping.

The sandstone and clayey limestone occur as lithified interbeds with no obvious relationship to the clays. The clayey limestone is a mudstone, according to the expanded classification of Dunham (Wilson, 1975) (i.e., very fine-grained and no obvious allochems). The sandstone is brownish gray, coarse- to fine-grained, having foraminifers, carbonate clasts with calpionellids, biotite, coalified plant debris, rock fragments, and feldspar as the major constituents. Sorting is poor. Some pieces of sand-

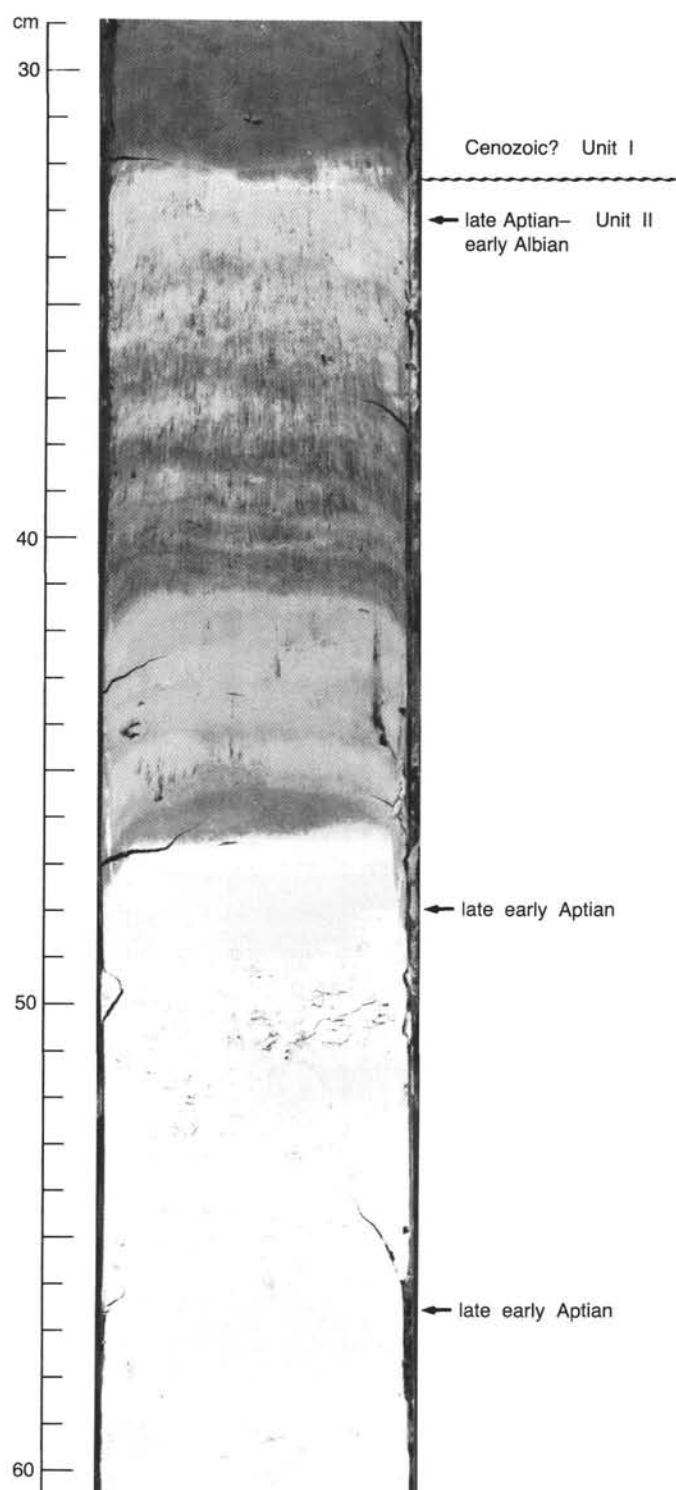


Figure 5. Sample 103-640A-2R-2, 29-60 cm. Lithologic Unit I/Unit II boundary is located at Sample 103-640A-2R-2, 32 cm.

stone show faint lamination and normally graded bedding ( $T_{a-b}$ ,  $T_{d-e}$ ). The sandstone is calcite cemented and cut by calcite veins.

All the cores from Subunit IIIB were fractured and disturbed by drilling. As in cores of similar sediments taken from Site 638 nearby, however, the drilling disturbance in Cores 103-640A-6R and 103-640A-7R has only magnified pre-existing deformation

from slumping. Cores 103-640A-8R and 103-640A-9R appear to be normally bedded, the bedding being nearly horizontal.

Subunit IIIB is interpreted as being a sequence of terrigenous turbidites and microturbidites, some of which were subsequently transported by slumping to their current location.

### BIOSTRATIGRAPHY

Foraminifers, nannofossils, and radiolarians were examined from sediments recovered at Hole 640A on the Iberian margin. A rare, poorly to moderately preserved deep-water agglutinated benthic foraminiferal assemblage was recovered from the brown clay of lithologic Unit I (Samples 103-640A-1R, CC, and 103-640A-2R-2, 30-32 cm; see "Sediment Lithology" section, this chapter) and indicates a Late Cretaceous age with deposition below the CCD. Nannofossils and radiolarians are absent from this unit. Sediments of the underlying lithologic Unit II (clayey ooze) contain benthic foraminifers of late Aptian/Albian age (Sample 103-640A-2R-2, 32-34 cm). More precisely, in Samples 103-640A-2R-2, 48-49 cm, 103-640A-2R-2, 56-58 cm, and 103-640A-2R-2, CC, planktonic foraminifers indicate an early Aptian age. Nannofossils and radiolarians recovered from this section indicate a middle Hauterivian to late Barremian age. The sandstone and limestone of lithologic Unit III contain a very rare and poorly preserved foraminiferal fauna, signifying late Hauterivian to Aptian age. A well-preserved and abundant nannofossil flora indicates a Hauterivian age in Cores 103-640A-5R to 103-640A-9R. Radiolarians recovered from lithologic Unit III similarly indicate Hauterivian to Aptian ages.

### Foraminifers

Generally rare, poorly to moderately well-preserved foraminifers occur sporadically in Hole 640A. Sample 103-640A-1R, CC, taken from the brown clay of lithologic Unit I, contains a few Neogene (mainly Miocene) planktonic contaminants, a few agglutinated benthic species (*Ammodiscus cretaceus*, *Paratrochamminoides* sp., and *Bathysiphon* sp.), and some Paleocene fish teeth (P. Doyle, pers. comm., 1985). Sample 103-640A-2R-2, 30-32 cm, just above the boundary between lithologic Units I and II, also contains a few agglutinants (*Hormosina ovulum*, *H. ovulum crassa*, *Plectrorecurvoides* sp., *Triplasia* sp., *Rhabdammina* sp., *Bathysiphon* sp.) and Cretaceous fish teeth but is devoid of Neogene calcareous contaminants. These *Rhabdammina*-like assemblages indicate a Late Cretaceous age (Krasheninnikov, 1974; Hemleben and Troester, 1984).

Clayey ooze in the uppermost part of lithologic Unit II contains middle Cretaceous impoverished assemblages. Sample 103-640A-2R-2, 33-34 cm, taken just below the discontinuity that defines the boundary between lithologic Unit I and Unit II, contains a few agglutinated benthic species. This low-diversity assemblage includes various species of *Bathysiphon* and trochamminids, *Glomospirella gaultina*, *Verneulinoides neocomiensis*, and a juvenile specimen of the calcareous benthic genus *Pleurostomella*. The co-occurrence of the two last taxa indicates a late Aptian/Albian age. A few centimeters below the discontinuity, Samples 103-640A-2R-2, 48-49 cm, and 103-640A-2R-2, 56-58 cm, provide a still more precise dating, based on late early Aptian (C13 Zone) planktonic assemblages, composed of small hedbergellids and globigerinelloids, including *Hedbergella sigali*, *H. sp. aff. planispira* (sensu Moullade), *H. similis* (sensu Longoria), *H. infracturea*, *H. gargasiana*, *Globigerinelloides blowi*, and *G. gottisi*. If the discontinuity between lithologic Units I and II coincides with the break-up unconformity (see "Seismic Stratigraphy" section, this chapter) separating the syn- and post-rift sequences, this age assignment is consistent with the dating of the same event at nearby DSDP Site 398 (Sibuet and Ryan, 1979).

Below this short fossiliferous interval, the rest of lithologic Unit II and lithologic Subunit IIIA are devoid of foraminifers,

except rare Neogene contaminants in core-catcher samples down to Core 103-640A-3R. Sample 103-640A-4R, CC, contains rare Lower Cretaceous agglutinated and calcareous (nodosariid) benthics, accompanied by rare planktonics, including Neogene contaminants and some Lower Cretaceous hedbergellids, having a poor preservation that precludes a better identification.

Lithologic Subunit IIIB cannot be dated on the basis of its foraminiferal content. Sample 103-640A-5R, CC, yields very rare non-age-diagnostic lenticulinids and nodosariids. Sample 103-640A-6R, CC, contains *Lenticulina ouachensis*, *Astacolus crepidularis*, and poorly preserved trocholines (*Trocholina* cf. *aptensis*, *T. infragranulata*), indicating a late Hauterivian to early Aptian age. Cores 103-640A-7R and 103-640A-8R are virtually barren of foraminifers and contain only extremely rare and tiny nodosariids or *Rhabdammina*-like agglutinated forms.

These impoverished foraminiferal assemblages, chiefly composed of tiny calcareous specimens, are thought to have been transported to Site 640 by turbidity currents, whereas the "primitive" agglutinated component is interpreted as being an *in-situ* microfauna. The absence of autochthonous calcareous benthic species implies that most if not all the section drilled at Hole 640A was deposited below or near the CCD.

### Nannofossils

Hauterivian to late Barremian nannofossil assemblages are present in sediment recovered from the only hole drilled at Site 640 (Cores 103-640A-2R through 103-640A-9R). The clays in Core 103-640A-1R through Sample 103-640A-2R-2, 47 cm, are barren. Nannofossil evidence indicates that part of the upper Hauterivian (and possibly some of the lower Barremian) is either absent or was not recovered between Cores 103-640A-4R and 103-640A-5R, which are dated according to nannofossil occurrence as early Barremian and early late Hauterivian. Upper Barremian sediment is in direct contact with upper Hauterivian sediment at Site 638.

Nannofossils are common to abundant in almost all Lower Cretaceous sediments. A decrease in abundance seen in Core 103-640A-9R is associated with an influx of silt-sized material. In general, preservation is moderate to excellent in claystone and poor to moderate in more calcareous-rich sediment.

Samples 103-640A-2R-2, 48–49 cm, through 103-640A-3R, CC, are dated as late Barremian and are assigned to the *Micrantholithus hoschulzii* Zone (CC-6; Sissingh, 1977). The absence of *Rucinolithus irregularis* and *Chiastozygus litterarius* in addition to the occurrence of *Haysites radiatus* in this interval is evidence of an age no younger than late Barremian.

Sample 103-640A-4R, CC, contains *Calcicalthina oblongata* and *Lithraphidites bollii* and is dated as early Barremian to late Hauterivian. *C. oblongata* is found at the top of Core 103-640A-4R; however, *L. bollii* is not observed above 103-640A-4R, CC. Cores 103-640A-5R through 103-640A-9R all contain assemblages that include *Calcicalthina oblongata*, *Lithraphidites bollii*, *Speetonia colligata*, *Cruciellipsis cuvieri*, and *Tubodiscus veranae*. This interval is assigned to the middle to late Hauterivian, *Cretarhabdus loriei* Zone (CC-4b).

### Radiolarians

Radiolarian preparations were made for all core-catcher samples from Hole 640A and for an additional 20 samples from Sections 103-640A-1R-1 to 103-640A-8R-1. Samples of lithologic Units I and II are barren of radiolarians and other siliceous microfossils. Samples from lithologic Unit III (Samples 103-640A-3R, CC, to 103-640A-8R, CC) are also barren, except Samples 103-640A-3R, CC, and 103-640A-5R, CC. Sample 103-640A-5R, CC, contains a few radiolarians preserved in pyrite; however, a strong crystal overgrowth with pyrite precludes determination of taxa. Sample 103-640A-3R, CC, contains an abun-

dant and well-preserved radiolarian assemblage recrystallized in pyrite. The fauna is diverse, and several age-diagnostic species could be distinguished, including *Sethocapsa uterculus*, *Triactoma* cf. *hyum*, *Archaeodictyomitra lacrimula*, *A. cf. vulgaris*, *Pseudodictyomitra lilyae*, *Xitus spicularis*, *Cyrtocapsa grutterinki*, *Alievum helenae*, *Thanarla pulchra*, *T. conica*, *Podobursa triacantha*, *Stichocapsa cribata*, *Willriedellum gilkeyi*, *Acaeniotyle diaphorogona*, *A. umbilicata*, *Angulobracchium* cf. *portmanni*, *Pantanellium lanceola*, *Pseudocrucella* sp., and *Acanthocircus diacranacanthos*. This assemblage characterizes the uppermost Hauterivian/lowest Barremian, but the absence of important marker species, which have their latest occurrence in the upper Hauterivian (*Siphocampium davidi* and *Sethocapsa trachyostaca*), suggests an early Barremian age for Sample 103-640A-3R, CC.

The age of this fauna coincides with the nannofossil data from Sample 103-640A-3R, CC (middle Barremian) and several samples of Core 103-640A-4R (early Barremian); the assemblage is also comparable, but slightly younger than Sample 103-638B-21R-1, 4–6 cm (early Barremian).

The overall faunal composition is somewhat strange; in fact, a large part of the age-diagnostic species is restricted to the 45–63- $\mu$ m size fraction, whereas the coarser fraction is dominated by non-diverse, long-ranging Spumellarids. In the western Tethys, radiolarian assemblages representing the time interval are characterized by the occurrence of large forms (*Podobursa*, *Obesacapsula*, *Mirifusus*), which are almost absent in Sample 103-640A-3R, CC. Whether this absence results from sorting during transport or from middle- to high-latitude areas being devoid of these genera is unclear. Because downward from Sample 103-640A-5R, CC, the sediments are mainly turbidites, the former explanation seems to be more likely.

### PALEOMAGNETICS

At Hole 640A, as at the previous holes, the whole-round paleomagnetic analyses measured only the degree of contamination by rust flakes and drilling slurry rather than the magnetization of the sediments (see "Explanatory Notes" chapter, this volume). Therefore, the following discrete oriented samples were taken for later shore-based analysis: 6 samples of brown clay in the upper 2 cores, 1 sample of Aptian(?) light-yellow clayey ooze (base of Core 103-640A-2R), and 20 samples of gray nannofossil marlstone and sandstone turbidites of Hauterivian–Barremian age. These samples were analyzed on a cryogenic magnetometer at the University of Wyoming, as described in the paleomagnetic report in the Site 638 chapter (this volume).

#### Brown Clay (Early Tertiary(?); Core 103-640A-1R through Sample 103-640A-2R-2, 32 cm)

The six samples were progressively thermally demagnetized to 550°C. Magnetization intensity was strong; natural remanent magnetization (NRM) intensities generally exceeded  $2 \times 10^{-5}$  emu/cm<sup>3</sup> ( $= 2 \times 10^{-2}$  A/m), and intensities at the 500°C step averaged about  $3 \times 10^{-6}$  emu/cm<sup>3</sup>. Characteristic directions were obtained from the 400° to 550°C steps. Two pairs of normal- and reversed-polarity zones are present (Fig. 6), although these are poorly documented. The lack of adequate age controls prevents any polarity chron assignments.

#### Marlstone and Sandstone Turbidites (Hauterivian–Aptian(?); Cores 103-640A-3R through 103-640A-9R)

Most of these samples have weak magnetization; intensities of characteristic magnetization average about  $2 \times 10^{-8}$  emu/cm<sup>3</sup>. The final polarity was apparent upon thermal demagnetization of 180°C or less, and characteristic directions of magnetization were generally obtained from 210° through 300°C. Un-



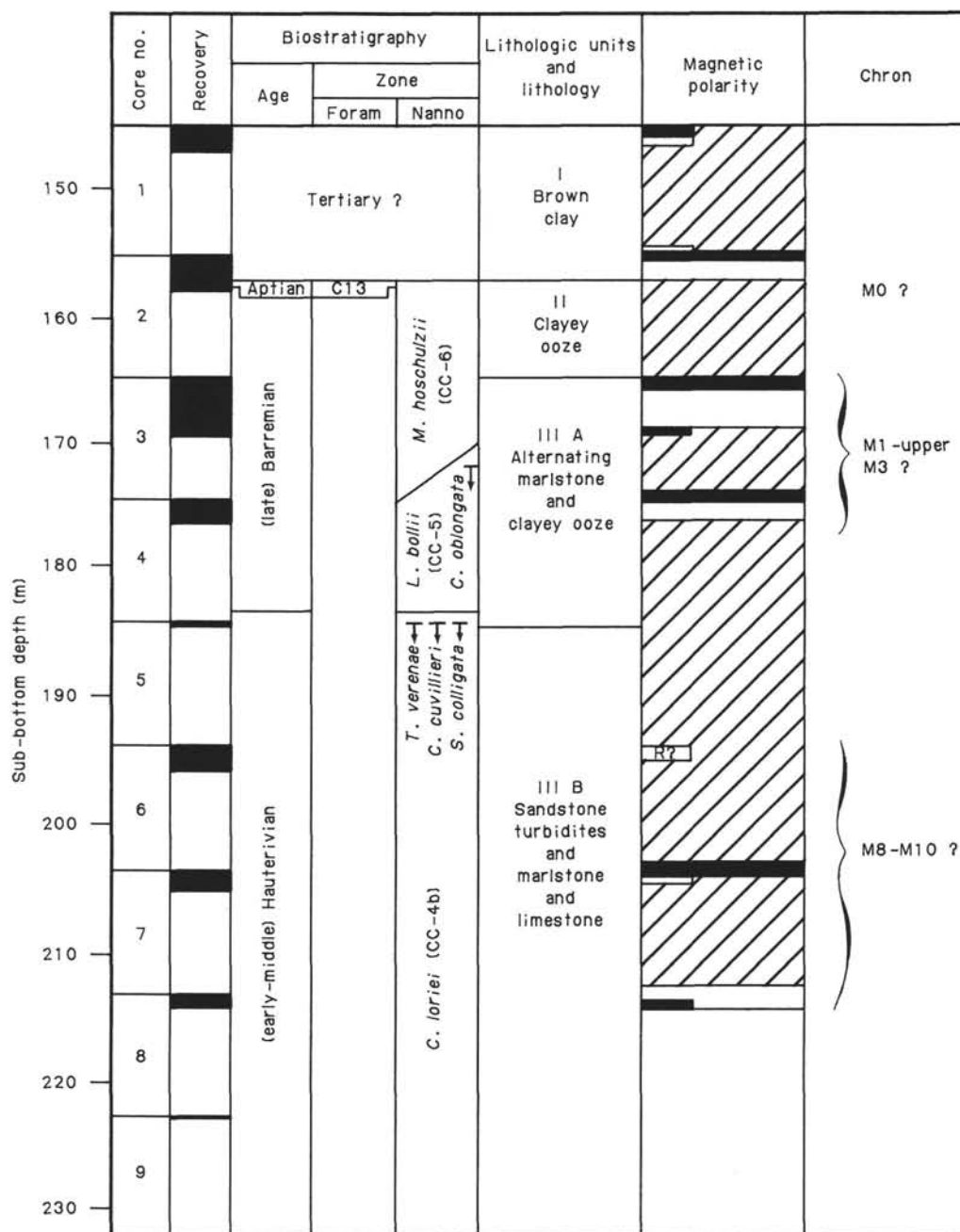


Figure 6. Magnetostratigraphy and tentative assignment of polarity chrons at Hole 640A. Black shading is normal-polarity zones, and white is reversed polarity. Diagonal pattern indicates gaps in recovery or intervals of indeterminant or unreliable polarity. Half bar represents single samples having a polarity interpretation opposite that of the adjacent samples or indicates that only one sample was available from the core. Assignment of magnetic polarity chrons is the best current guess based upon the polarity time scales. Complete tables of the paleomagnetic data and polarity interpretations will be given in Part B of the Leg 103 volumes.

stable or viscous magnetizations were commonly exhibited at about 300°C. The few samples of sandstone or claystone turbidites had strong and more stable magnetization.

Sparse core recovery coupled with slow sedimentation rate rendered the determination of a reliable magnetostratigraphy difficult (Fig. 6). Tentative polarity chron assignments are based mainly on the nannofossil datums, using the magnetic polarity time scale compiled by Ogg (in press). The nannofossil datums are all highest occurrences of key species and, hence, are possibly affected by redeposition in this turbidite-rich sequence.

The sample of light-yellow clayey ooze has reversed polarity and, therefore, could correspond to polarity chron M0 if the Aptian-age determination made aboard ship is correct. The late Barremian has predominately reversed polarity, which could correspond to polarity chron M1 and/or upper M3 of that age. As at Site 638, the early Barremian and the latest Hauterivian appears to be absent. The sparse recovery of the middle Hauterivian yielded mixed polarity, but detail is inadequate to enable assignment of these zones to the polarity chrons between M8 and M10 of this age interval. Better guesses about the correlation of



the polarity zones to polarity chrons will be possible when the dinoflagellate biostratigraphy is available.

## ORGANIC GEOCHEMISTRY

### Organic Carbon Analysis

Ten samples were taken at Site 640 for organic carbon and nitrogen determination using the Perkin-Elmer elemental analyzer. Results of the organic carbon percentage on a dry-sediment weight basis and percentage of carbonate are listed in Table 3. Because of technical problems, reliable determination of elemental nitrogen was not possible.

Samples recovered at Site 640 are similar to those recovered at Site 638 (see "Sediment Lithology" sections, this chapter and Site 638 chapter). For a complete discussion of the character of the organic matter, see "Organic Geochemistry" section in the Site 638 chapter (this volume).

### Organic Carbon Isotope Analysis

Organic carbon isotope values are listed in Table 4.

## INORGANIC GEOCHEMISTRY

### Interstitial-Water Chemistry

Two sediment samples were taken from the rotary-drilled cores recovered at Site 640 and were squeezed aboard ship to obtain the interstitial water from the sediment. The water samples were analyzed for pH, alkalinity, chlorinity, salinity, calcium, and magnesium. The same analytical methods used at the previous sites on Leg 103 were employed for analysis of the interstitial waters obtained at Site 640. The primary standard used for calibration of the water analysis is IAPSO standard seawater, and surface seawater retrieved by a bucket overboard was used for comparison with the interstitial water.

The results listed in Table 5 are similar to the results obtained from similar sub-bottom depths at other Leg 103 sites. Calcium values at Site 640 are slightly higher than those obtained from the other sites, but the general trends of an increase in calcium concentration and a decrease in magnesium concentration with increasing sub-bottom depth remains the same. The pH remains relatively constant, and the alkalinity decreases with increasing sub-bottom depth. The decrease in alkalinity in the lower sample from Site 640 (Sample 103-640A-7R-1, 140–150 cm; 204.7 m sub-bottom depth) may be associated with the increasing lithification and carbonate precipitation in the sandstone, limestone, and marlstone microturbidites of lithologic Subunit IIIB.

### Calcium Carbonate

Nineteen samples were analyzed for percentage of carbonate; results are listed in Table 6 and graphed in Figure 7. Lithologic Unit I, composed of brown clay, contains no carbonate in the dried-sediment samples. Lithologic Unit II is characterized by clayey ooze but also contains clay and marl as minor lithologies. The carbonate values in three samples from lithologic Unit II range from 6% to 69% of the dried-sediment weight. Lithologic Subunit IIIA consists of marlstone and clayey ooze having carbonate values that range from 46% to 89% of the dried-sediment weight. Lithologic Subunit IIIB, having a wider range, 13%–89%, in the percentage of carbonate of the dried-sediment weight than does the overlying Subunit IIIA, consists of sandstone, limestone, and marlstone microturbidites.

## PHYSICAL PROPERTIES

Physical-property measurements were made on sediments and sedimentary rocks from Hole 640A according to the procedure outlined in previous site reports of Leg 103, except as noted here. After the cores were sectioned and logged into the core inventory records, bulk density of core sections was continuously

Table 3. CHN summary, Site 640.

Sample (interval in cm)	Sub-bottom depth (m)	Organic carbon (%)	Inorgan. carbon (%)	Lithology	Lithologic unit
103-640A-1R-1, 60–62	146.0	0.11	0	Brown clay	I
103-640A-3R-1, 140–142	166.41	1.06	46	Marl	IIIA
103-640A-3R-3, 140–142	169.10	0.98	65	Marl	IIIA
103-640A-3R-4, 12–14	169.32	0.10	88	Clayey ooze	IIIA
103-640A-4R, CC, 5–7	176.18	0.15	63	Marlstone	IIIA
103-640A-5R, CC, 4–6	184.27	0.93	36	Marlstone	IIIA
103-640A-6R-1, 48–50	194.18	1.02	13	Calcareous clay	IIIB
103-640A-7R-1, 20–22	203.50	0.10	63	Marl	IIIB
103-640A-7R-1, 84–86	204.14	0.99	21	Calcareous clay	IIIB
103-640A-8R-1, 38–40	213.38	1.09	23	Calcareous claystone	IIIB

Table 4. Organic carbon isotope values, Hole 640.

Sample	Sub-bottom depth (m)	Age	Organic carbon (%)	CaCO <sub>3</sub> (%)	$\delta^{13}\text{C}$
103-640A-3R-1, 140–142	166.41	Barremian	1.06	46	–27.6
103-640A-5R, CC, 4–6	184.27	Barremian	0.93	36	–23.8
103-640A-6R-1, 48–50	194.18	Barremian	1.02	13	–25

Table 5. Shipboard interstitial-water analyses, Site 640.

Sample (interval in cm)	Sub-bottom depth (m)	pH	Alkalinity (meq/kg)	Salinity (‰)	Chlorinity (‰)	Ca <sup>++</sup> (mmol/L)	Mg <sup>++</sup> (mmol/L)
103-640A-3R-2, 140–150	167.7	7.57	2.40	34.1	19.16	15.58	43.49
103-640A-7R-1, 140–150	204.7	7.56	1.92	34.2	19.29	18.24	38.51

Table 6. Carbonate-bomb data, Site 640.

Sample (interval in cm)	Sub-bottom depth (m)	Carbonate (%)	Lithology <sup>a</sup>
103-640A-1R-1, 60-62	146.0	0	Brown clay
103-640A-2R-1, 100-102	156.1	0	Brown clay
103-640A-2R-2, 41-42	157.01	6	Light-olive clay
103-640A-2R-2, 57-58	157.17	69	Clayey nannofossil ooze
103-640A-2R, CC, 18-20	157.40	42	Marl
103-640A-3R-1, 140-142	166.1	46	Marl
103-640A-3R-2, 21-22	166.41	89	Clayey nannofossil ooze
103-640A-3R-2, 138-140	167.58	81	Clayey ooze
103-640A-3R-3, 140-142	169.1	65	Marl
103-640A-3R-4, 12-14	169.32	88	Clayey ooze
103-640A-4R-1, 15-17	174.45	65	Marl
103-640A-4R, CC, 5-7	176.18	63	Marlstone
103-640A-5R, CC, 4-6	184.27	36	Marlstone
103-640A-6R-1, 48-50	194.18	13	Calcareous clay
103-640A-6R-1, 131-133	195.01	89	Clayey limestone
103-640A-7R-1, 20-22	203.5	63	Marl
103-640A-7R-1, 84-86	204.14	21	Calcareous clay
103-640A-7R, CC, 6-8	204.98	62	Fine-grained calcareous sandstone
103-640A-8R-1, 38-40	213.38	23	Calcareous claystone

<sup>a</sup> Lithologic names are those used on visual core description forms.

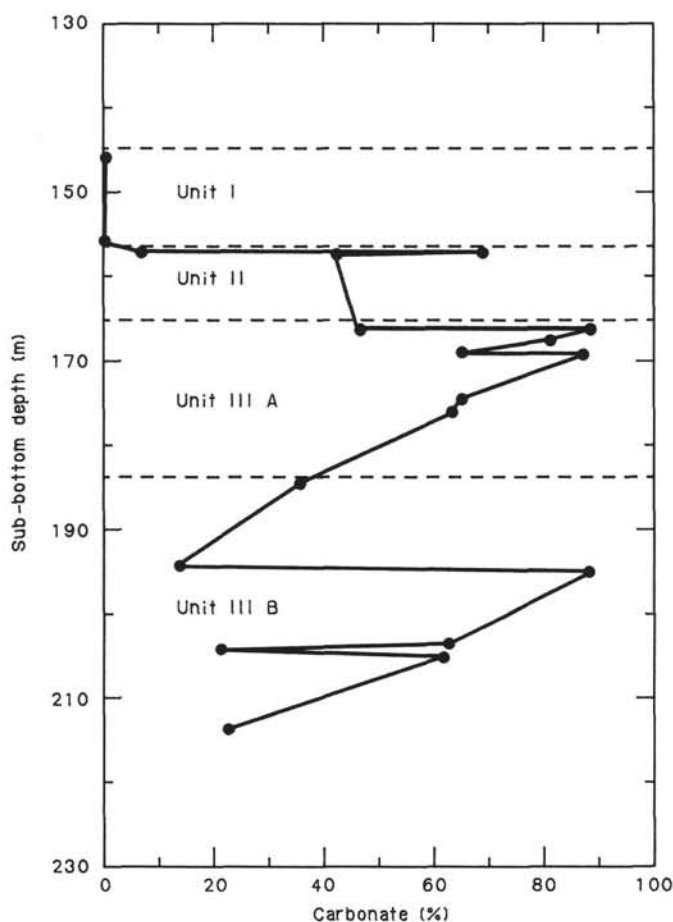


Figure 7. Percentage of carbonate in dried-sediment samples from Site 640. Boundaries of the lithologic units are superimposed. Data are given in Table 6.

measured on the Gamma Ray Attenuation Porosity Evaluator (GRAPE). The cores were then allowed to warm for 4 hr to stable room temperature before sediment was analyzed for thermal conductivity. After this, the sections were split and sampled for further physical-property measurements. Because Hole 640A be-

gan with a washed interval, the contents of Core 103-640A-1R (145.4-155.1 m sub-bottom) were already too stiff for measurement of shear strength without damaging the vane-shear-strength apparatus. Compressional seismic velocity of sediments and sedimentary rock from Hole 640A was measured on the Hamilton Frame velocimeter, and these same samples were measured gravimetrically for index properties (bulk and grain density, water content, and porosity), using a triple-beam balance for weight and the Penta-Pycnometer for volume. Bulk-density values by 2-min GRAPE measurements and percentage of carbonate composition by carbonate-bomb analyses (Müller and Gastner, 1971) were also made on these samples.

### Thermal Conductivity

Thermal-conductivity measurements were made on unlithified sediments from Cores 103-640A-1R through 103-640A-8R (145.4-222.5 m sub-bottom; Fig. 8A). Thermal conductivity increases linearly with sub-bottom depth from  $2.4$  to  $3.9 \times 10^{-3} \text{ cal} \times ^\circ\text{C}^{-1} \times \text{cm}^{-1} \times \text{s}^{-1}$  (calories/degree Celsius-centimeter-second).

### Compressional Velocity

Compressional seismic velocities were measured on sediments and sedimentary rocks from Cores 103-640A-1R through 103-640A-8R (145.4-222.5 m sub-bottom; Fig. 8B). The two samples from lithologic Unit I (stiff brown mud; Core 103-640A-1R through Sample 103-640A-2R-2, 32 cm; 145.4-156.9 m sub-bottom; see "Sediment Lithology" section, this chapter) average  $1.67 \text{ km/s}$ . A single sample of clayey ooze from lithologic Unit II (Samples 103-640A-2R-2, 32 cm, through 103-640A-2R, CC; 156.9-164.7 m sub-bottom) yields a seismic velocity of  $1.65 \text{ km/s}$ . Seismic velocities of four unlithified samples and one limestone sample were measured from lithologic Subunit IIIA (Core 103-640A-3R through Sample 103-640A-5R-1, 4 cm; 164.7-184.4 m sub-bottom). The unlithified marl and clayey ooze yield velocities of  $1.48$ - $1.85 \text{ km/s}$ ; the limestone velocity is  $3.3 \text{ km/s}$ . Marl and sandstone from lithologic Subunit IIIB (Samples 103-640A-5R-1, 4 cm, through 103-640A-9R, CC; 184.4-232.2 m sub-bottom) have seismic velocity ranges of  $1.7$ - $1.8 \text{ km/s}$  and  $3.5$ - $5.7 \text{ km/s}$ , respectively. Although the number of samples from each lithologic unit is too small to show reliable trends with depth, examination of Figure 8B reveals a slight increase in seismic velocity of unlithified sediment with depth. Values reported have a precision of  $\pm 0.02 \text{ km/s}$ .

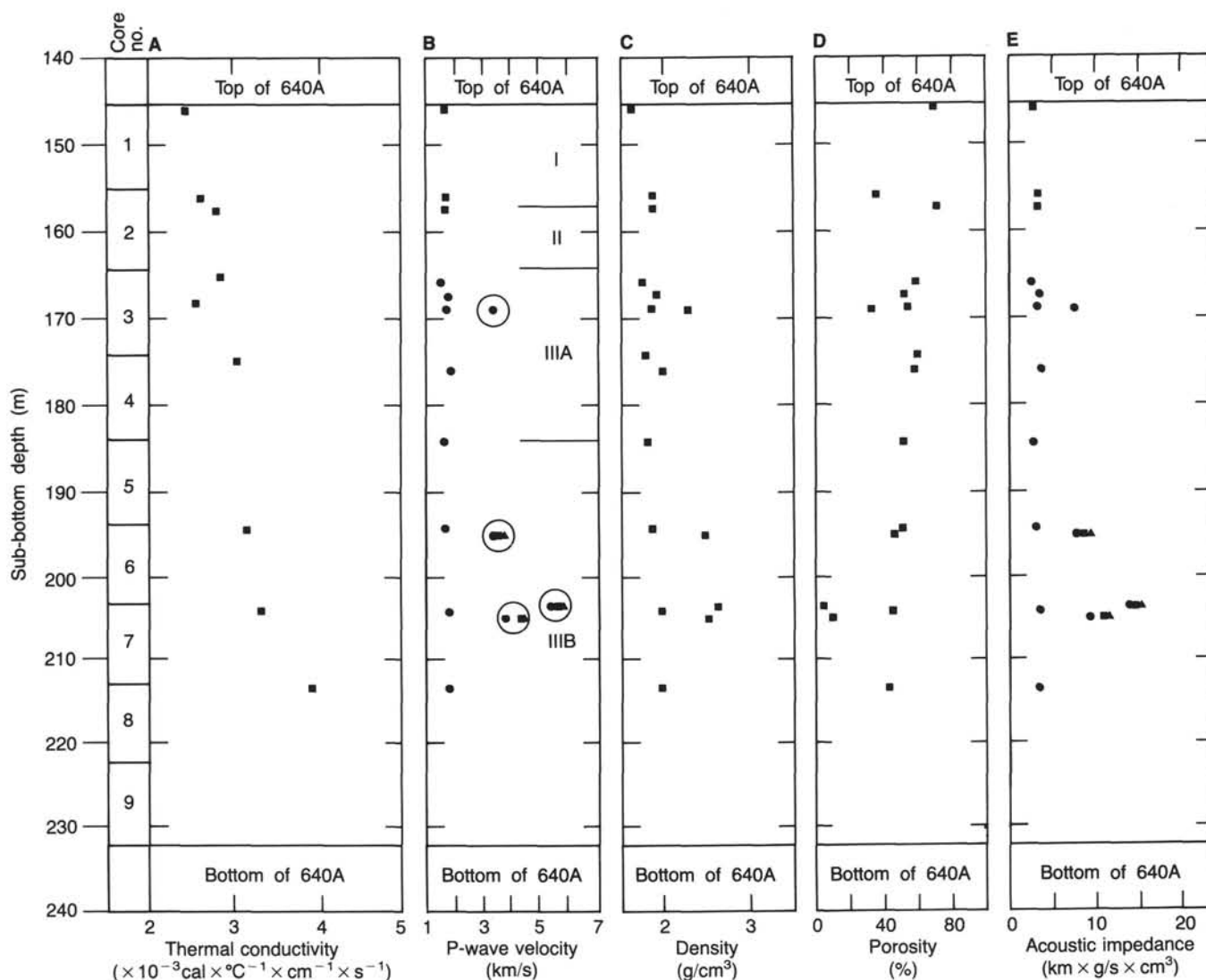


Figure 8. Physical-property measurements on sediments and sedimentary rocks from Hole 640A plotted against sub-bottom depth. Lithologic units as described in the "Sediment Lithology" section (this chapter) are indicated on the right side of the seismic-velocity column. A. Thermal-conductivity values ( $\times 10^{-3} \text{ cal} \times ^\circ\text{C}^{-1} \times \text{cm}^{-1} \times \text{s}^{-1}$ ). B. Compressional seismic velocity (kilometers per second). Square data points indicate velocities measured in the plane of the core diameter and parallel to the cut face of the core (c-direction); triangular data points indicate velocities measured in the plane of the core diameter and perpendicular to the cut face of the core (b-direction), and dots indicate velocities measured perpendicular to the plane of the core diameter (a-direction). Cemented-rock data points (limestone and sandstone) are encircled. C. Bulk density (grams per cubic centimeter). D. Porosity (percent). E. Acoustic impedance (compressional velocity  $\times$  bulk density;  $\text{km} \times \text{g/s} \times \text{cm}^3$ ). Data point symbols same as in B.

The proportion of limestone and sandstone is difficult to estimate because of low core recovery; thus, its significance in generating a reflector is not clear. By tabulating the occurrence and velocity of lithified sediment from the shipboard visual core descriptions and assuming that unrecovered material consists of marl, we calculate an average seismic velocity of 1.80 km/s for lithologic Subunit IIIB.

### Index Properties

Bulk density and porosity of the brown clay of lithologic Unit I (two samples) average 1.75 g/cm<sup>3</sup> and 53%, respectively (Figs. 8C and 8D). The single sample from lithologic Unit II has a bulk density of 1.88 g/cm<sup>3</sup> and a porosity of 71%. Bulk density and porosity of unlithified clayey ooze and marl from lithologic Subunit IIIA (five samples) average 1.9 g/cm<sup>3</sup> and 55%, respectively, and bulk density and porosity of the single limestone sample from Subunit IIIA (Sample 103-640A-3R-4, 12–14 cm; 169.1 m sub-bottom) is 2.3 g/cm<sup>3</sup> and 33%, respectively. Unlithified marl from Subunit IIIB (four samples) averages a

bulk density of 2.0 g/cm<sup>3</sup> and a porosity of 50%; lithified sandstone (three samples) averages a bulk density of 2.6 g/cm<sup>3</sup> and a porosity of 8%. As with seismic velocity, the number of samples in any unit is too small to show trends with depth, but examination of Figures 8C and 8D indicates that unlithified sediments show an overall slight increase in bulk density and decrease in porosity.

Figure 9 depicts bulk density plotted against compressional seismic velocity. The unlithified sediments show a slight increase in seismic velocity and bulk density with increasing depth; the cemented sandstone and limestone samples show a greater increase in seismic velocity with increase in bulk density.

### Acoustic Impedances and Possible Reflectors

There is no reason to expect a large or abrupt acoustic impedance contrast between lithologic units at Site 640 until the occurrence of sandstone in lithologic Subunit IIIB (top of Subunit IIIB is at 184.4 m sub-bottom). On the basis of Neogene-ooze drill chippings at the top of Core 103-640A-1R and by

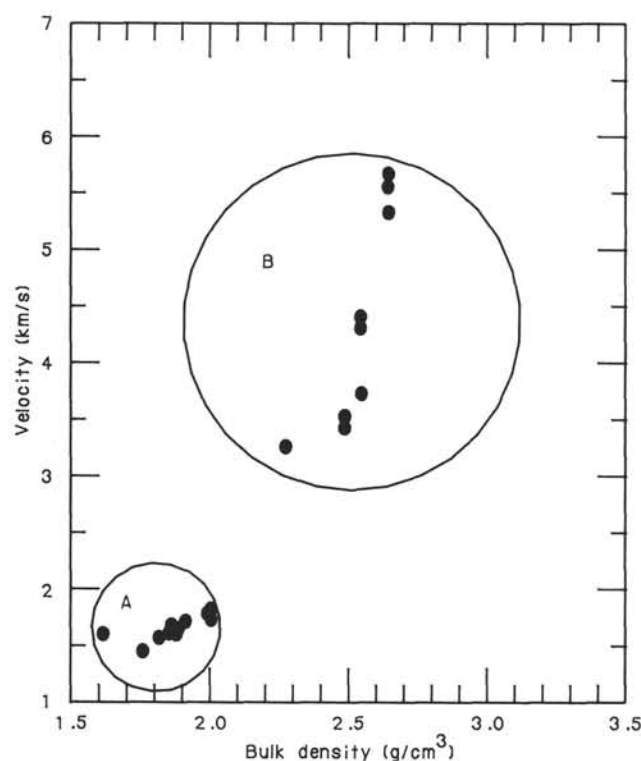


Figure 9. Bulk density ( $\text{g/cm}^3$ ) plotted against compressional seismic velocity ( $\text{km/s}$ ) for Hole 640A. The set of data points within area A corresponds to unlithified sediments, which show a slight increase in seismic velocity and bulk density with greater depth. The set of data points in area B corresponds to cemented sandstone and limestone, which show a greater increase in seismic velocity with increase in bulk density.

analogy with Sites 637, 638, and 639, where Neogene ooze overlies the undated brown mud, we assumed that Neogene ooze overlies lithologic Unit I at Site 640 and calculated a reflection coefficient for the interface of Neogene ooze and lithologic Unit I. If the material washed through was the Neogene calcareous ooze characterizing the surface sediment at other sites, it should have physical properties similar to those measured at the other sites. From Table 7 in the "Physical Properties" section of the Site 638 chapter (this volume), typical seismic-velocity, bulk-density, and acoustic-impedance values of the regional Neogene ooze are  $1.65 \text{ km/s}$ ,  $2.00 \text{ g/cm}^3$ , and  $3.30 \text{ km-g/s-cm}^3$ , respectively. The brown mud of lithologic Unit I in Hole 640A has a typical seismic velocity, bulk density, and acoustic impedance of  $1.67 \text{ km/s}$ ,  $1.75 \text{ g/cm}^3$ , and  $2.92 \text{ km-g/s-cm}^3$  (Fig. 8E). The reflection coefficient of the interface of these sediment types is

$0.061$ , which seems rather low to have generated the upper reflector in the regional seismic profile.

Because the reflectivity between ooze and lithologic Unit I brown clay is small, we calculated the reflectivity ( $R$ ) of the interface between other lithologic units to explore other possible locations of the reflector interface, using the equation

$$\frac{V_{p1}\rho_{b1} - V_{p2}\rho_{b2}}{V_{p1}\rho_{b1} + V_{p2}\rho_{b2}}$$

where  $V_p$  is compressional seismic velocity ( $\text{km/s}$ ) and  $\rho_b$  is bulk density ( $\text{g/cm}^3$ ). Table 7 lists average velocities, bulk densities, acoustic impedances (the product of compressional seismic velocity and bulk density), and calculated reflectivity ( $R$ ) between each of the lithologic units.

None of the calculated reflectors is high, probably owing to an artifact of low recovery. At Site 640, material similar in age and lithology to that of Site 638 was recovered. Site 640 is more distant from terrigenous sediment sources than is Site 638; the lithologic unit comparable to Site 640 lithologic Subunit IIIB (Site 638 lithologic Subunit IIIB; Site 638 chapter, this volume) contains a more significant proportion of sandstone than was recovered at Site 640 and generated a strong reflector based on both calculations of physical properties and of logging. We suspect that this lithologic Subunit IIIB is the site of the upper acoustic reflector at Site 640.

### Summary

Thermal conductivity increases steadily with depth from  $2.4$  to  $3.9 \times 10^{-3} \text{ cal} \times ^\circ\text{C}^{-1} \times \text{cm}^{-1} \times \text{s}^{-1}$  in Hole 640A. Measured seismic velocity increases slightly with depth from an average velocity of  $1.67 \text{ km/s}$  in lithologic Unit I to  $1.80 \text{ km/s}$  in lithologic Unit III. Bulk density also increases slightly from  $1.75$  to  $2.03 \text{ g/cm}^3$ , and porosity decreases, although not as steadily, from  $53\%$  in lithologic Unit I through  $71\%$  in lithologic Unit II,  $55\%$  in Subunit IIIA, and  $50\%$  in Subunit IIIB.

Physical properties and recovered proportions of different lithologies indicate that reflection coefficients between the lithologic units of Site 640 are rather low. We suspect that the material drilled but not recovered in Hole 640A includes sandstone in sufficient proportion in lithologic Subunit IIIB to generate the reflector observed in the seismic profile at this site.

### AGE-VS.-DEPTH CURVE

The data on the biostratigraphic age of samples from Site 640 are displayed on Figure 10, arranged according to their depths below the seafloor. No samples were obtained in the fossiliferous part of the Cenozoic rock, and the brown clay overlying Aptian beds in Cores 103-640A-1R and 103-640A-2R is barren of fossils. The remaining fossiliferous part of the section is Early Cretaceous in age, but, as shown in Figure 10, the age

Table 7. Average seismic velocity ( $V_p$ ), bulk density ( $\rho_b$ ), and acoustic impedance ( $V_p\rho_b$ ) of lithologic units of Hole 640A and calculated reflectivity ( $R$ ) between lithologic units.

	$V_p$ ( $\text{km/s}$ )	$\rho_b$ ( $\text{g/cm}^3$ )	$V_p\rho_b$	$R$
Neogene ooze <sup>a</sup>	1.65	2.06	3.30	0.061 ooze/I
Unit I (brown clay)	1.67	1.88	2.92	0.029 I/II
Unit II (clayey ooze)	1.65	1.88	3.10	0.022 II/IIIA
Subunit IIIA (Lower Cretaceous marlstone/ooze)	1.71	1.90	3.24	0.060 IIIA/IIIB
Subunit IIIB (Lower Cretaceous marlstone, sandstone, limestone)	1.80	2.03	3.65	

<sup>a</sup> Neogene ooze was not recovered at Hole 640A but is interpreted to occur in the washed interval from 0–145.4 m sub-bottom, according to drilling results from other Leg 103 sites.



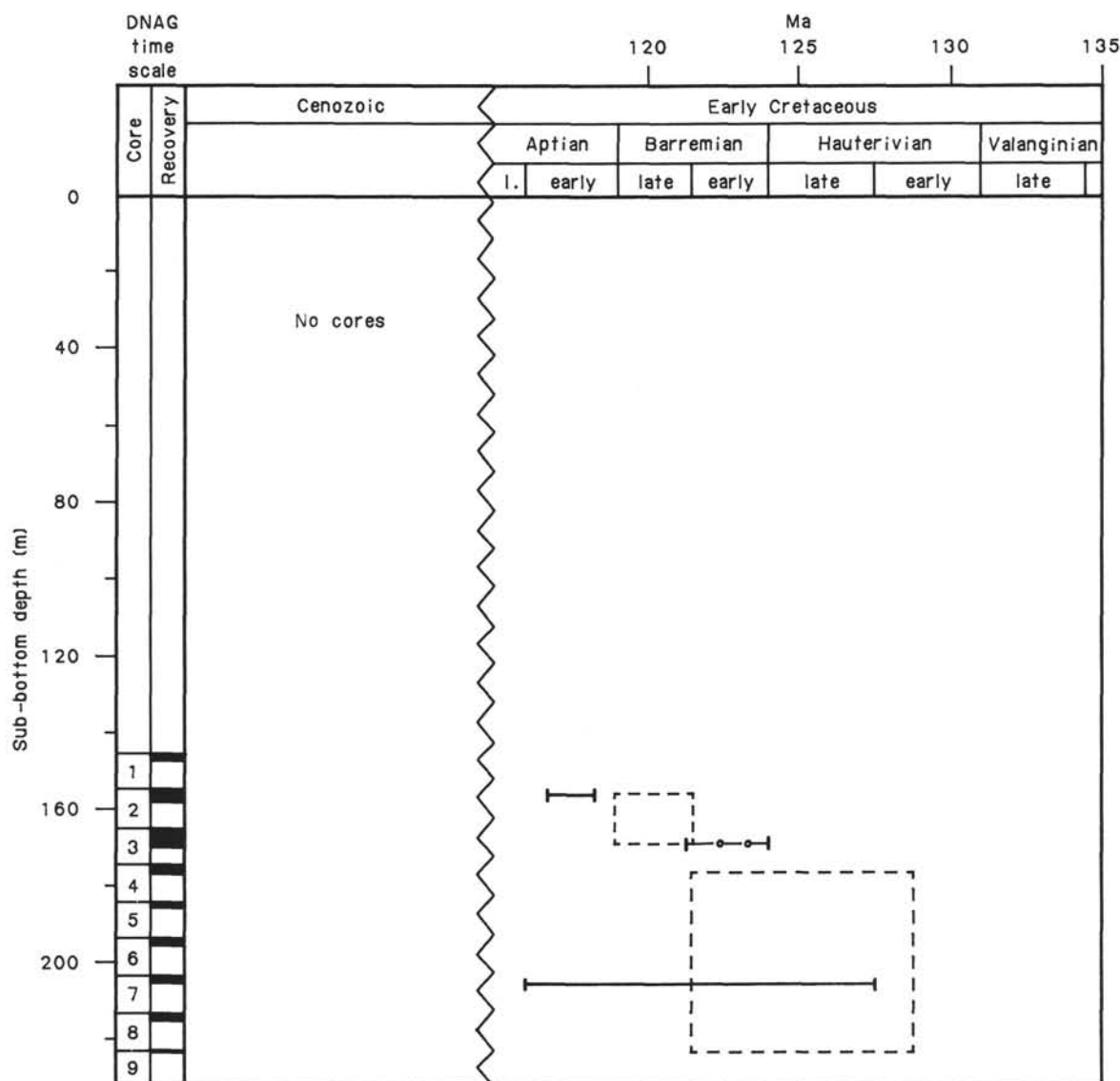


Figure 10. Age-vs.-depth curve, Site 640 (Hole 640A). Foraminiferal data are shown by solid lines, nannofossil data by dashed lines, and radiolarian data by a dash-circle line.

ranges of the fossils are too large to allow reliable estimates of the rates of sedimentation or accumulation.

### SEISMIC STRATIGRAPHY

Site 640 is on the top of a ridge in an area where the S reflector is both strong and continuous (see "Background and Objectives" section, this chapter) but where the seismic units between S and the reflector identified as being the mid-Cretaceous break-up unconformity show little coherence of internal reflectors. The Neogene cover over the ridge is thin; 200 ms of two-way travelt ime was recorded on both the multichannel seismic line and on the seismic line from the *JOIDES Resolution* during the site survey. Lower Cretaceous marl, assumed to be the top of the acoustically incoherent unit, was reached about 165 m below the seafloor, implying a seismic velocity in the underlying sediment of 1.6 km/s, coinciding well with the velocity measured on core samples (see "Physical Properties" section, this chapter).

The main result of drilling at Site 640 was to identify the uppermost part of the acoustically incoherent unit as being Lower Cretaceous marlstone, siltstone, and sandstone much like sediments drilled at Site 638. Comparison of the seismic stratigra-

phy at Sites 640 and 638 shows one difference and one similarity of great importance:

1. The difference: Lower Cretaceous syn-rift sediments are well layered on seismic profiles at Site 638 but nearly incoherent at Site 640 (Fig. 11). Although the cores from Site 640 show no greater degree of slumping and faulting than those from Site 638, we assume that, on the average, the syn-rift sequence is more broken and disturbed at Site 640 than at Site 638.

2. The similarity: At both sites, syn-rift Cretaceous sediments rest on a strong and continuous reflector. At Site 638, the reflector is identified as being the top of dolomite and/or Tithonian limestone. In the basin east of Site 638, in the deeper part of the half graben, the thickness of the syn-rift sequence is about 3 km, assuming a seismic velocity of 3.5 km/s. At Site 640, the thickness of the diffracting layer resting upon the S reflector is also 3 km, assuming the same velocity. Thus, the S reflector is in a position analogous to the strong reflector at the top of the carbonates at Sites 638 and 639 and is tentatively correlated either with the top of carbonates or with crystalline basement. In any case, the result of drilling at Site 640 may preclude the previous interpretation that the S reflector marks the duc-

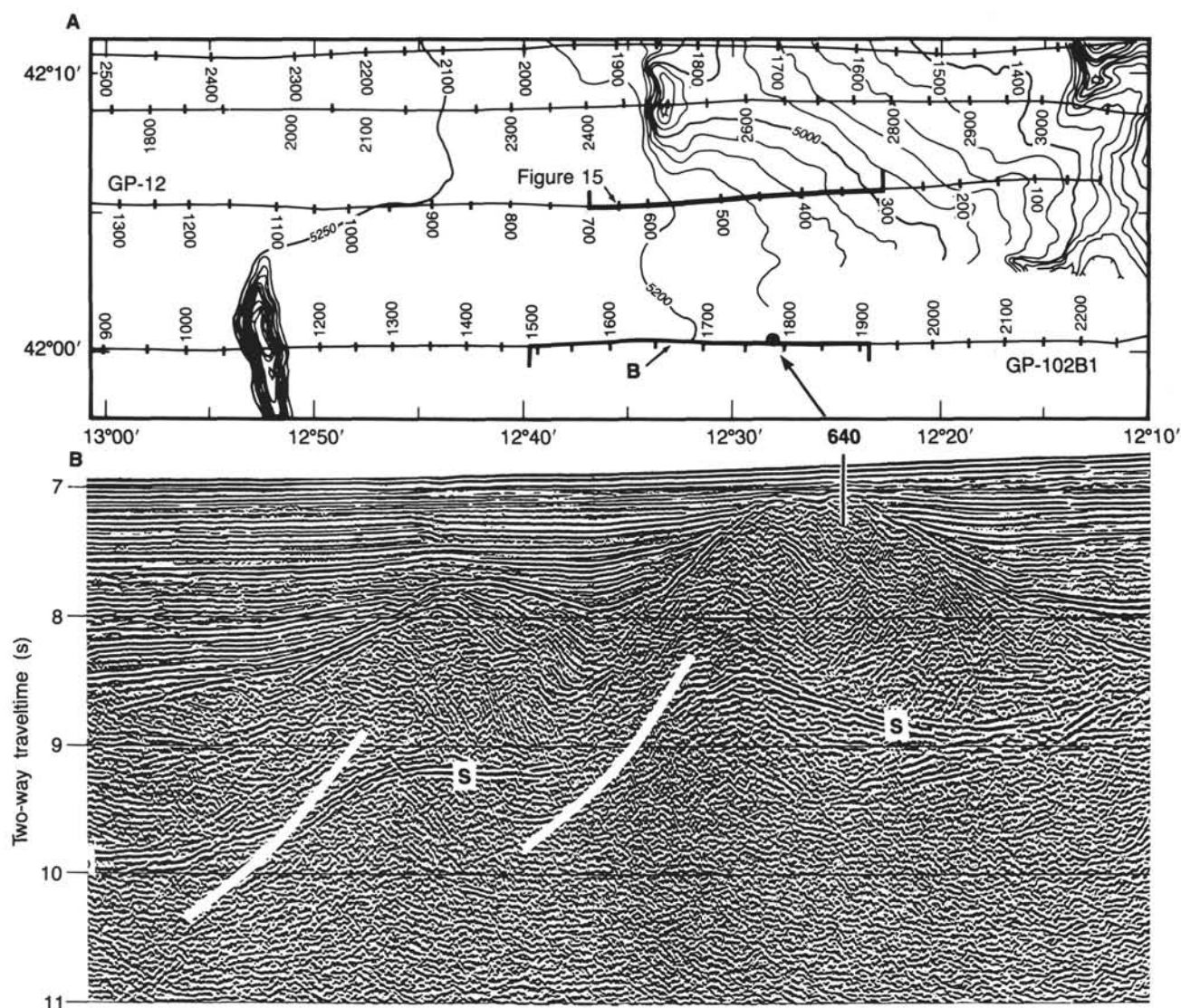


Figure 11. A. Sea Beam map (courtesy of J. C. Sibuet). Locations of Site 640, of the seismic line shown in B, and of seismic line shown in Figure 15 are shown. B. IFP seismic line GP-102B1 (courtesy of L. Montadert) and location of Site 640. S = reflector S, assumed to be collapsed by two normal faults.

tile/brittle boundary in the continental crust (see “Background and Objectives” section, this chapter).

The broad undulations in the S reflector persist when we draw a cross section using a velocity of 1.7 km/s for post-rift and 3.5 km/s for syn-rift strata. The steep limbs of the reflector undulations may be the result of normal faults that offset pre-rift rocks (Fig. 11).

Drilling at Site 640 also investigated the break-up unconformity. At Site 398 (Leg 47B), near Vigo Seamount, this unconformity is probably latest Aptian in age (Sibuet, Ryan, et al., 1979). At Site 640, lower Aptian marlstone is included in the sequence below the break-up unconformity, which is therefore necessarily younger. The data from the two sites, thus, agree well.

## SUMMARY AND CONCLUSIONS

### Objectives at Site 640

Drilling at Site 640 was mainly to gain an understanding of not only the sedimentary and tectonic history of Galicia mar-

gin, in particular, but also the mechanisms of formation of passive continental margins, in general. We questioned whether the deep and strong reflector—the S reflector—seen on multichannel seismic-reflection profiles that cross the foot of Galicia margin is, as proposed by Montadert et al. (1979) for the Armorican margin and extended by Chenet et al. (1982) to the Galicia margin, the boundary surface created within the continental, silicic crystalline basement during Cretaceous thinning of the crust between an upper crust that was brittle and deformed by faulting and a lower crust that was ductile and deformed more plastically. The alternative hypothesis is that the S reflector is not within the basement but is either at the top of a high-impedance sedimentary layer, e.g., carbonate rocks, or is at the top of crystalline basement.

The resemblance between seismic profiles of the American and Galicia margins is striking (Fig. 12). In both places, a ridge composed of a vaguely layered, acoustically complex seismic unit, ranging from about 0.5 to 1.5 s in thickness, rests on a strong, smooth, and continuous reflector. The acoustically complex layer is overlain by the distinctive, acoustically transparent

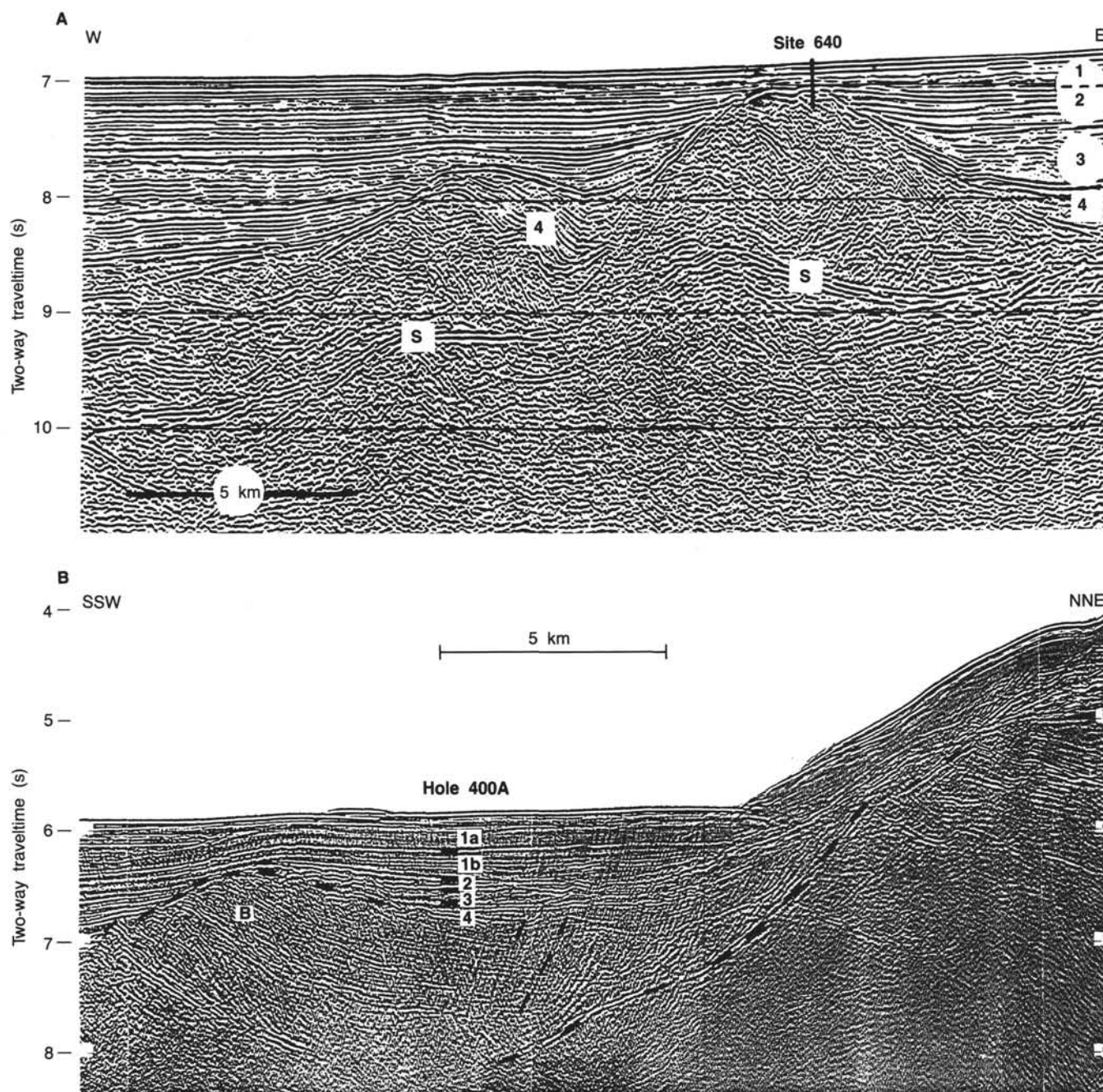


Figure 12. A. Multichannel seismic-reflection profile IFP GP-102B1, from shotpoints 1470 to 1900. Site 640 is near this line. 1, 2, 3: post-rift sediments; 3: post-Aptian black shale; 4: syn-rift, Lower Cretaceous sediments. S: S reflector. Courtesy of L. Montadert. B. Multichannel seismic profile IFP-CNEXO-CEPM OC 412 across Hole 400A on the Armorican margin on the northeast side of the Bay of Biscay. The original caption of this figure (fig. 4 in Montadert et al., 1979) identifies the units as 1a-1b = post-Eocene Cenozoic, 2 = Upper Cretaceous to Eocene, 3 = Aptian/Albian, 4 = syn-rift sediments, and B = pre-rift sediments.

post-rift black shale. Montadert et al. (1979) and Chenet et al. (1982), interpreted the acoustically complex unit as being pre-rift sedimentary strata of Early Cretaceous and older ages. Our finding, however, at Site 638 of a great thickness of Lower Cretaceous syn-rift sediments above the strong reflector identified at Site 639 as the top of the Upper Jurassic/lowest Cretaceous carbonate platform indicates that drilling at Site 640 could provide a test of the two hypotheses, that is, whether the acoustically complex unit above the strong reflector consists of pre-rift or syn-rift sediments.

### Stratigraphy of Sequence Cored at Site 640

The lithology, biostratigraphy, and key physical properties of the section cored at Site 640 appear in graphic form in Figure 13. The following discussion summarizes the salient features of the sequence, from oldest to youngest.

#### *Lower Cretaceous Strata (Lithologic Units II and III)*

A thickness of about 48 m of sandstone-claystone-marlstone turbidites of Hauterivian age occurs in the lowest interval cored

Location: 42°00.7'N, 12°27.8'W    Water depth: 5201 m below derrick floor (5191 mbsl)

Depth	Core	Rec.	Graphic lith.	Description	Age	Biostratigraphy			P-wave velocity (km/s)			Density (g/cm <sup>3</sup> )		
						Foraminifers	Nannofossils	Other	2	3	4	1.5	2.0	2.5
10	Drilled interval				Probably Neogene									
20														
30														
40														
50														
60														
70														
80														
90														
100														
110														



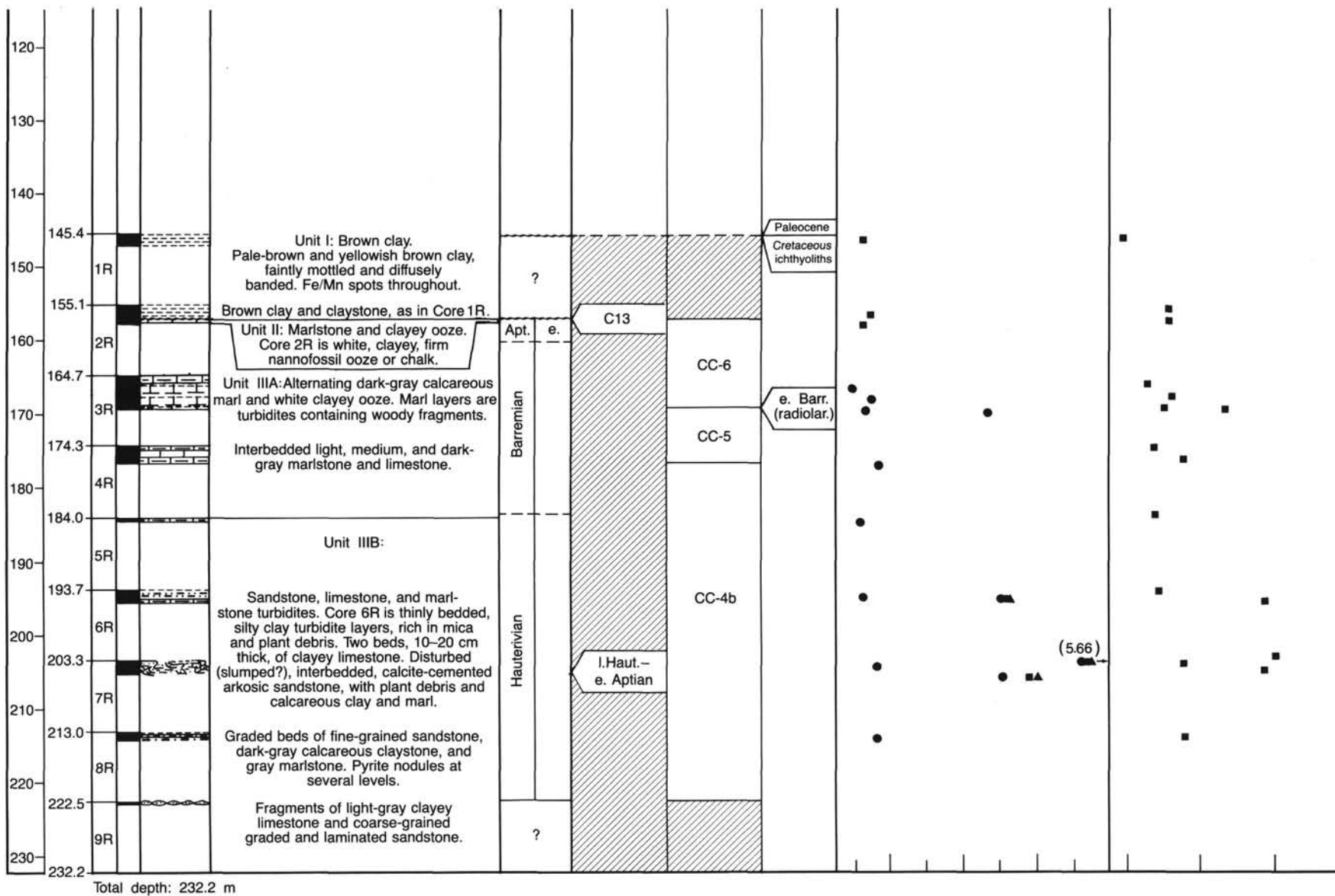


Figure 13. Summary logs, Site 640 (Hole 640A). Explanation of symbols in P-wave velocity column is given in Figure 8B.

at Site 640 and passes upward into about 28 m of marlstone and clayey ooze of Hauterivian, Barremian, and early Aptian age. The sandy turbidite sequence is similar to the Hauterivian and Valanginian turbidite sequence at Site 638 in bedding style, sedimentary structures, mineralogy, cementation, and abundance of resedimented terrestrial plant debris. The overlying marlstone and claystone are likewise similar in lithology to the Hauterivian, Barremian, and lower Aptian beds cored at Site 638. The difference between the sequences at the two sites is that at Site 640 the sandstone beds may occur at slightly younger levels than does the bulk of the sandstone at Site 638.

#### **Cretaceous and Paleogene Brown Clay (Lithologic Unit I)**

Brown clay rests directly on lower Aptian marlstone, but the upper limit of this unit is in the washed interval above the top of the first core. Minimum thickness is 11.5 m. The clay has vague, diffuse banding and is somewhat mottled in shades of yellowish and pale brown. Small dark spots of iron/manganese oxide dot the clay everywhere. The clay contains no calcium carbonate.

The clay resembles the brown clay cored between the peridotite and Neogene ooze at Site 637 and the brown clay sampled between the dolomite and Neogene ooze at Hole 639C. The age of these clay intervals is only loosely constrained by the presence of ichthyoliths; ichthyoliths at this site are assigned by P. Doyle (pers. comm., 1985) to the Paleocene (at 147 m) and the Cretaceous (at 157 m).

As shown in Figure 14, comparable unfossiliferous brown clay occurs at several other drill sites in the North Atlantic, where the dating of overlying and underlying beds constrains the age as being probably Paleogene and possibly late Paleocene to Eocene, a time when the regional CCD was probably at a relatively shallow depth (Laughton, Berggren, et al., 1972; Sibuet, Ryan, et al., 1979).

#### **Neogene Sediments**

No cores were taken in the upper sediments at Site 640 because the upper Neogene had been continuously cored at Site 637. The physiography of the layers seen on the seismic profile (Fig. 3) suggests that they are mainly distal turbidites, as at Site 637.

#### **Discussion**

The discovery of Lower Cretaceous turbidite sandstone, marlstone, and claystone similar to the strata that constitute the syn-rift sequence at Site 638, viewed in the context of the features seen on the multichannel seismic-reflection profile across the area of Site 640, suggests that the acoustically incoherent unit above the S reflector at least partly consists of a thick sequence of syn-rift turbidites. Study of the seismic profile (Fig. 3) reveals that between S and the break-up unconformity at the base of seismic unit 3, two units exist: an upper, fairly well-stratified unit, labeled unit 4 on Fig. 3, and a lower, poorly stratified,

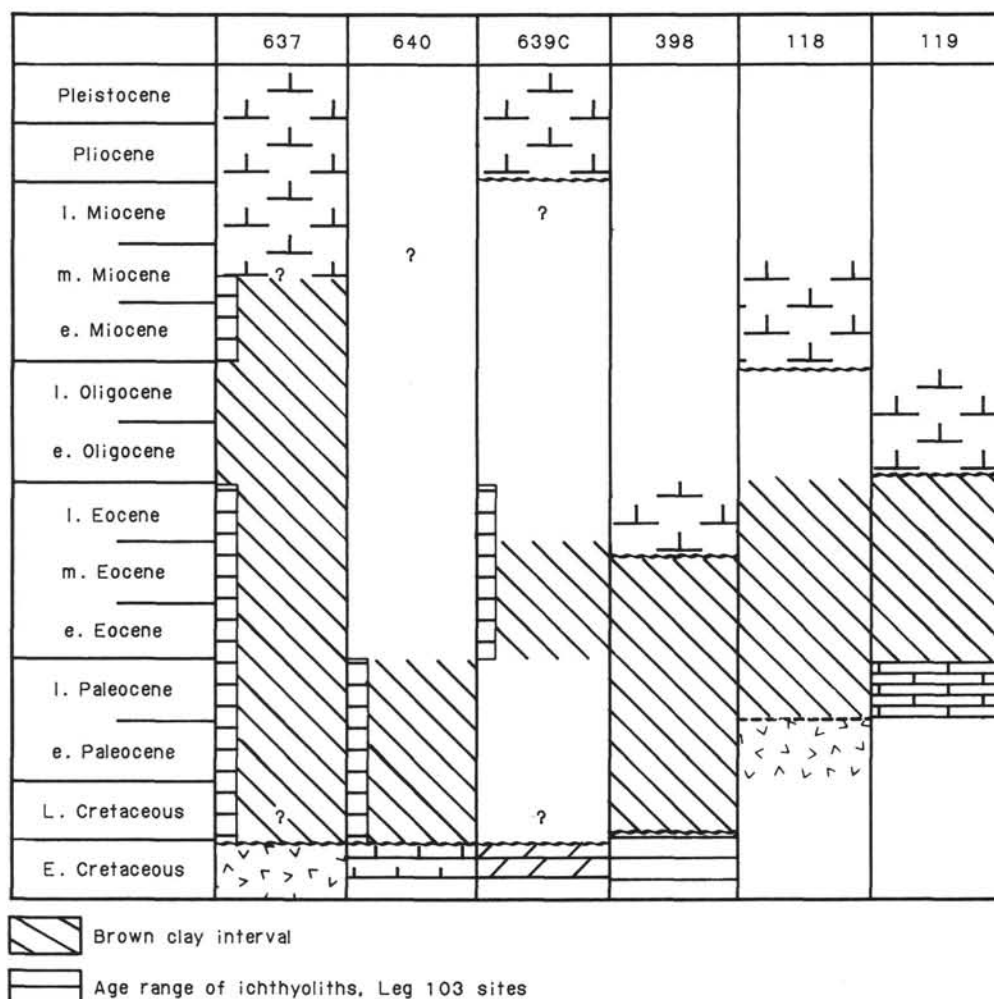


Figure 14. Occurrences of brown clay at North Atlantic DSDP and ODP drill sites.

complex unit that lies immediately beneath the Cenozoic east of Site 640. Within the lower unit, intermittent reflectors are present, but only near the west end of the profile in Fig. 3 are these reflections consistently traceable over distances of more than about 1 km.

Another multichannel seismic profile (Fig. 15) along a line parallel to the profile through Site 640 and about 9 km north of the site shows the S reflector and the layering in the overlying sediments. Syn-rift beds beneath the two buried hills dip east, and the dip appears to increase eastward. The S reflector, especially beneath the eastern side of the eastern buried hill, appears to dip more gently than does the overlying strata, possibly because the reflector may be, at least locally, a low-angle detachment surface separating the syn-rift sequence from underlying carbonates and basement. The undulating form of the S reflector on this profile is partly due to the velocity "turn-down" effects of the post-rift sediments in the troughs between buried hills.

One of the characteristic features of the S reflector is its smoothness, i.e., its lack of local relief. This contrasts with the form of the reflection at the top of the carbonate platform, e.g., on the seismic line that passes near Sites 638, 639, and 641 (Fig. 16). There, and on all the profiles that cross the two half grabens where dredging indicates that carbonate-platform rocks underlie the syn-rift sediments, the reflector at the top of the carbonate strata shows a small-scale roughness distinctively different from the smooth surface shown by the S reflector.

The combined evidence from drilling and seismic data suggests that the S reflector may be overlain by a thick sequence of Lower Cretaceous syn-rift sediments. Even though the reflector would thus be at the level of the top of the carbonate platform, or perhaps of the crystalline basement, its smooth form suggests that it may be a low-angle detachment fault developed along the former depositional contact.

## REFERENCES

- Boillot, G., 1986. Comparison between the Galicia and Aquitaine margins. *Tectonophysics*, 129:243-255.
- Boillot, G., Auxietre, J. L., Dunand, J. P., Dupeuble, P. A., and Mauffret, A., 1979. The northwestern Iberian margin: a Cretaceous passive margin deformed during Eocene. In Talwani, M., Hay, W. W., and Ryan, W. B. F., (Eds.), *Deep Drilling Results in the Atlantic Ocean: Continental Margins and Paleoenvironment, Maurice Ewing Series*: Washington (Am. Geophys. Union), 3:138-153.
- Boillot, G., Grimaud, S., Mauffret, A., Mougenot, D., Mergoil-Daniel, J., Kornprobst, J., and Torrent, G., 1980. Ocean-continent boundary off the Iberian margin: a serpentine diapir west of the Galicia Bank. *Earth and Planet Sci. Lett.* 48:23-34.
- Chenet, P., Montadert, L., Gairaud, H., and Roberts, D., 1982. Extension ratio measurements on the Galicia, Portugal, and northern Biscay continental margins: implications for evolutionary models of passive continental margins. In Watkins, J. S., and Drake, C. L. (Eds.), *Studies in Continental Margin Geology*: Am. Assoc. Pet. Geol. Mem., 34:703-715.
- de Graciansky, P. C., Poag, C. W., et al., 1985. *Init. Repts. DSDP*, 80: Washington (U.S. Govt. Printing Office).
- Hemleben, C., and Troester, J., 1984. Campanian-Maestrichtian deep-water foraminifers from Hole 543A, Deep Sea Drilling Project. In Biju-Duval, B., Moore, J. C., et al., *Init. Repts. DSDP*, 78A: Washington (U.S. Govt. Printing Office), 509-532.
- Krasheninnikov, V. A., 1974. Upper Cretaceous benthonic agglutinated foraminifera, Leg 27 of the Deep Sea Drilling Project, In Veevers, J. J., Heirtzler, J. R., et al., *Init. Repts. DSDP*, 27: Washington (U.S. Govt. Printing Office), 631-662.
- Laughton, A. S., Berggren, W. A., Benson, R. N., Davies, T. A., Franz, U., Musich, L. F., Perch-Nielsen, K., Ruffman, A. S., van Hinte, J. E., Whitmarsh, R. B., Aumento, F., Clarke, A. D., Ryall, P. J. C., Cann, J. R., Bryan, W. B., and Bukry, D., 1972. Site 118. In Laughton, A. S., Berggren, W. A., et al., *Init. Repts. DSDP*, 12: Washington (U.S. Govt. Printing Office), 673-751.
- Masson, D. G., Montadert, L., and Scrutton, R. A., 1985. Regional geology of the Goban Spur continental margin. In de Graciansky, P. C., Poag, C. W., et al., *Init. Repts. DSDP*, 80: Washington (U.S. Govt. Printing Office), 1115-1139.
- Maurry, R. C., Bellon, H., Bougault, H., Joron, J. L., Bohn, M., and de Graciansky, P. C., 1985. Oceanic tholeiites from Leg 80 sites (Celtic Sea passive margin, northeastern Atlantic): geochemistry and mineralogy. In de Graciansky, P. C., Poag, C. W., et al., *Init. Repts. DSDP*, 80: Washington (U.S. Govt. Printing Office), 939-946.
- Montadert, L., Roberts, D. G., De Charpal, O., and Geunne, P., 1979. Rifting and subsidence of the northern continental margin of the Bay of Biscay. In Montadert, L., and Roberts, D., et al., *Init. Repts. DSDP*, 48: Washington (U.S. Govt. Printing Office), 1025-1060.
- Müller, G., and Gastner, M., 1971. The "Karbonate-Bombe," a simple device for determination of the carbonate content in sediments, soils, and other materials. *Neues Jahrb. Mineral. Monatsch.*, 10: 466-469.
- Ogg, J. C., in press. Early Cretaceous magnetostratigraphy, DSDP Sites 534 and 603, western North Atlantic. In van Hinte, J., Wise, S., et al., *Init. Repts. DSDP*, 93: Washington (U.S. Govt. Printing Office).
- Sibuet, J. C., and Ryan, W. B. F., 1979. Site 398: evolution of the West Iberian passive continental margin in the framework of the early North Atlantic Ocean. In Sibuet, J. C., Ryan, W. B. F., et al., *Init. Repts. DSDP*, 47, Pt. 2: Washington (U.S. Govt. Printing Office), 761-775.
- Sibuet, J. C., Ryan, W. B. F., et al., 1979. *Initial Reports of the Deep Sea Drilling Project*, 47, Pt. 2: Washington (U.S. Govt. Printing Office).
- Sissingh, W., 1977. Biostratigraphy of Cretaceous calcareous nannoplankton. *Geol. Mijnbouw*, 56:37-65.
- Wilson, J. L., 1975. *Carbonate Facies in Geologic History*. New York (Springer Verlag).

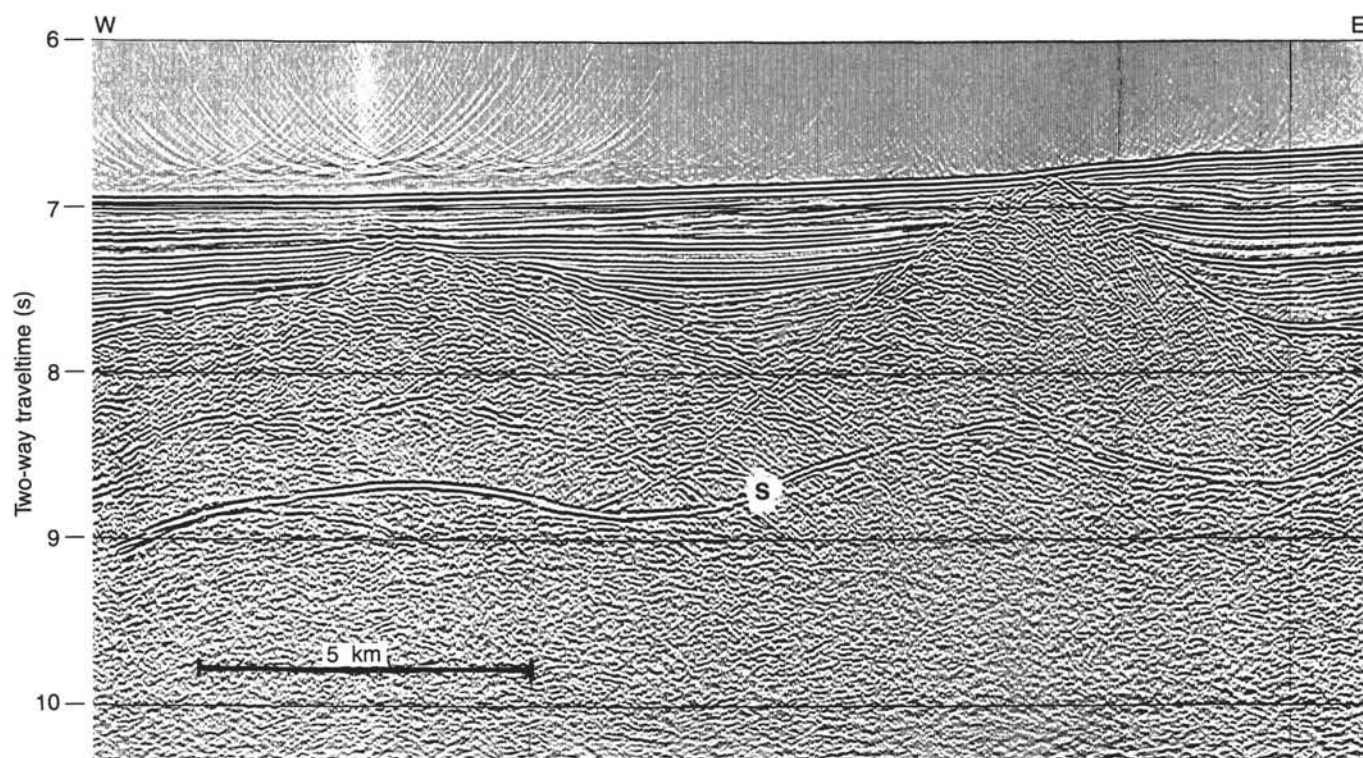


Figure 15. Multichannel seismic line GP-12, from shotpoints 300 to 700. The line is about 9 km north of Site 640, and the higher of the two buried hills is along the same ridge on which Site 640 is located. Note the smooth form of the strong reflector between 8 and 9 s of two-way reflection time. Courtesy of L. Montadert. Location of profile is shown in Figure 11A.



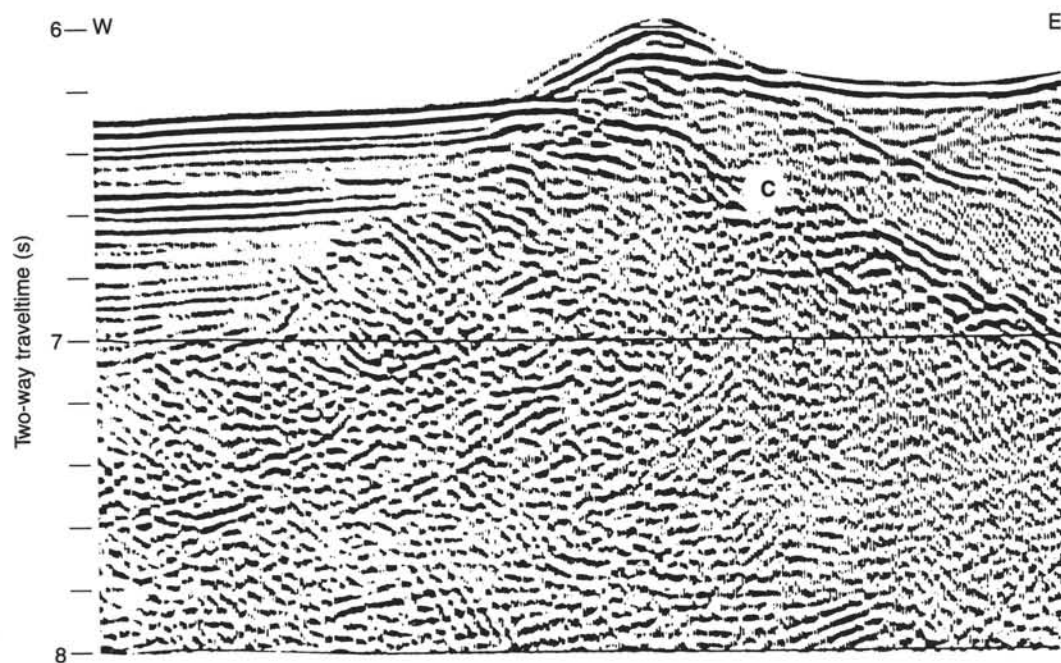
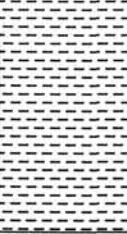
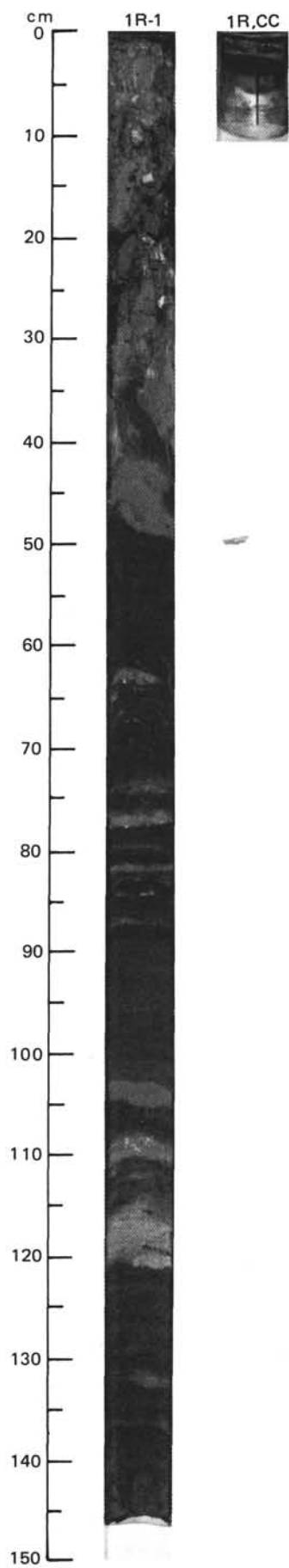


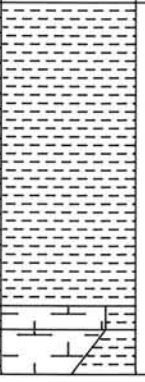

Figure 16. Multichannel seismic line GP-101, which passes near Sites 638, 639, and 641. Note the somewhat irregular form of the strong reflector marking the sedimentary contact at the top of the carbonate platform, marked "C" on the figure.

SITE 640 HOLE A CORE 1 R CORED INTERVAL 5335.9-5345.6 mbsl; 145.4-155.1 mbsf

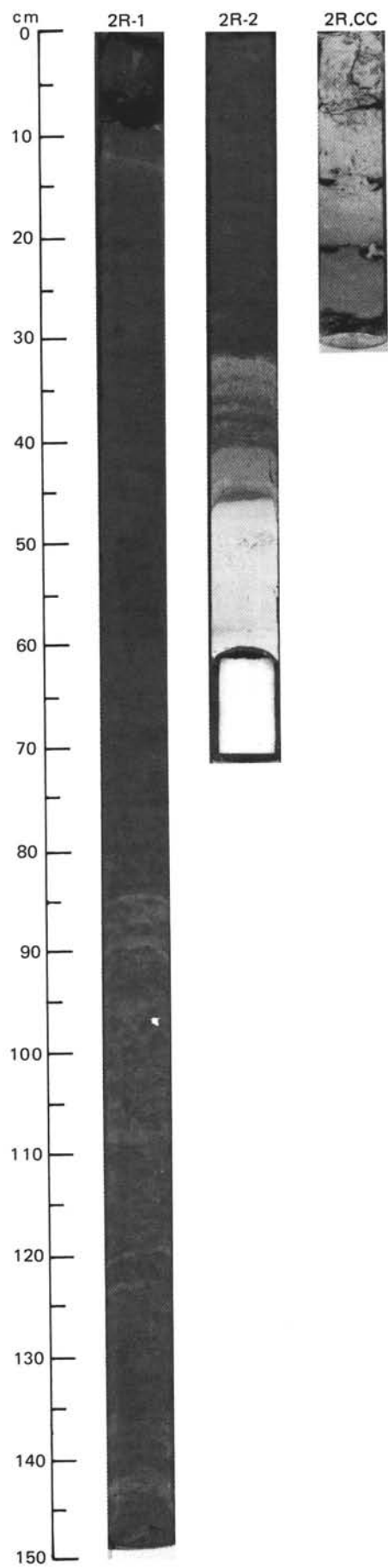
TIME-ROCK UNIT	BIOSTRAT. ZONE/ FOSSIL CHARACTER				PALEOMAGNETICS	PHYS. PROPERTIES	CHEMISTRY	SECTION	METERS	GRAPHIC LITHOLOGY	DRILLING DISTURB.	SED. STRUCTURES	SAMPLES	LITHOLOGIC DESCRIPTION																																																																																																														
	FORAMINIFERS	NANNOFOSSILS	RADIOLARIANS	DIATOMS																																																																																																																								
TERTIARY?	M12-13 (downhole contamination) R/P	B					0 %	1	0.5 1.0		O O		* * * * *	<p><b>BROWN CLAY.</b></p> <p>The core consists of pale brown (10YR6/3, 10YR7/4) and yellowish brown (10YR3.5/2) clay, faintly mottled and with diffuse banding. Very dark gray (10YR3/1) spots 0.1-0.6 cm across, rich in organic matter or Fe/Mn oxide occur throughout. The top 35 cm of the core are cavings and drilling slurry incorporating fragments of clay and white marl.</p> <p><b>SMEAR SLIDE SUMMARY (%):</b></p> <table><tr><td></td><td>1,15</td><td>1,26</td><td>1,48</td><td>1,56</td><td>1,119</td><td>CC</td></tr><tr><td></td><td>M</td><td>M</td><td>D</td><td>D</td><td>D</td><td>D</td></tr></table> <p><b>TEXTURE:</b></p> <table><tr><td>Silt</td><td>10</td><td>40</td><td>2</td><td>13</td><td>10</td><td>2</td></tr><tr><td>Clay</td><td>90</td><td>60</td><td>98</td><td>87</td><td>90</td><td>98</td></tr></table> <p><b>COMPOSITION:</b></p> <table><tr><td>Quartz</td><td>15</td><td>—</td><td>2</td><td>4</td><td>—</td><td>—</td></tr><tr><td>Mica</td><td>4</td><td>—</td><td>—</td><td>—</td><td>—</td><td>—</td></tr><tr><td>Clay</td><td>90</td><td>25</td><td>94</td><td>87</td><td>95</td><td>95</td></tr><tr><td>Volcanic Glass</td><td>—</td><td>—</td><td>Tr</td><td>—</td><td>—</td><td>—</td></tr><tr><td>Calcite/Dolomite</td><td>1</td><td>—</td><td>4</td><td>5</td><td>—</td><td>1</td></tr><tr><td>Accessory Minerals</td><td>Tr</td><td>—</td><td>Tr</td><td>3</td><td>5</td><td>4</td></tr><tr><td>Foraminifers</td><td>—</td><td>5</td><td>—</td><td>—</td><td>—</td><td>—</td></tr><tr><td>Nannofossils</td><td>—</td><td>70</td><td>Tr</td><td>—</td><td>—</td><td>1</td></tr><tr><td>Fish Remains</td><td>—</td><td>—</td><td>Tr</td><td>—</td><td>—</td><td>—</td></tr><tr><td>Organic matter</td><td>—</td><td>—</td><td>—</td><td>2</td><td>—</td><td>—</td></tr></table> <p><b>PHYSICAL PROPERTIES DATA:</b></p> <table><tr><td></td><td>1,60</td><td>1,61</td></tr><tr><td>V<sub>ρ</sub> (c)</td><td>—</td><td>1.64</td></tr><tr><td>ρ<sub>b</sub></td><td>—</td><td>1.62</td></tr><tr><td>T<sub>c</sub></td><td>2.43</td><td>—</td></tr></table>		1,15	1,26	1,48	1,56	1,119	CC		M	M	D	D	D	D	Silt	10	40	2	13	10	2	Clay	90	60	98	87	90	98	Quartz	15	—	2	4	—	—	Mica	4	—	—	—	—	—	Clay	90	25	94	87	95	95	Volcanic Glass	—	—	Tr	—	—	—	Calcite/Dolomite	1	—	4	5	—	1	Accessory Minerals	Tr	—	Tr	3	5	4	Foraminifers	—	5	—	—	—	—	Nannofossils	—	70	Tr	—	—	1	Fish Remains	—	—	Tr	—	—	—	Organic matter	—	—	—	2	—	—		1,60	1,61	V <sub>ρ</sub> (c)	—	1.64	ρ <sub>b</sub>	—	1.62	T <sub>c</sub>	2.43	—
	1,15	1,26	1,48	1,56	1,119	CC																																																																																																																						
	M	M	D	D	D	D																																																																																																																						
Silt	10	40	2	13	10	2																																																																																																																						
Clay	90	60	98	87	90	98																																																																																																																						
Quartz	15	—	2	4	—	—																																																																																																																						
Mica	4	—	—	—	—	—																																																																																																																						
Clay	90	25	94	87	95	95																																																																																																																						
Volcanic Glass	—	—	Tr	—	—	—																																																																																																																						
Calcite/Dolomite	1	—	4	5	—	1																																																																																																																						
Accessory Minerals	Tr	—	Tr	3	5	4																																																																																																																						
Foraminifers	—	5	—	—	—	—																																																																																																																						
Nannofossils	—	70	Tr	—	—	1																																																																																																																						
Fish Remains	—	—	Tr	—	—	—																																																																																																																						
Organic matter	—	—	—	2	—	—																																																																																																																						
	1,60	1,61																																																																																																																										
V <sub>ρ</sub> (c)	—	1.64																																																																																																																										
ρ <sub>b</sub>	—	1.62																																																																																																																										
T <sub>c</sub>	2.43	—																																																																																																																										



SITE 640 HOLE A CORE 2 R CORED INTERVAL 5345.6-5355.2 mbsl; 155.1-164.7 mbsf

TIME-ROCK UNIT	BIOSTRAT. ZONE/ FOSSIL CHARACTER				PALEOMAGNETICS	PHYS. PROPERTIES	CHEMISTRY	SECTION	METERS	GRAPHIC LITHOLOGY	DRILLING DISTURB.	SED. STRUCTURES	SAMPLES	LITHOLOGIC DESCRIPTION
	FORAMINIFERS	NANNOFOSSILS	RADIOLARIANS	DIATOMS										
TERTIARY?	B	C 13 (blow Zone) F/PR/MF/PR/P					0 %	1	0.5 1.0				*	BROWN CLAYSTONE and CLAYEY NANNO OOZE.  The core consists of faintly banded, firm, brown (10YR4/2) clay or claystone overlying firm, greenish white (5Y8/1) clayey nanno ooze or chalk. The two lithologies are separated by a 15 cm band of olive gray (5Y7/2) clay with many blue-black laminae and streaks in the upper 10 cm and limonitic yellow patches up to 0.5 cm across. The brown clay has mottled appearance with many darker patches, but no clear burrowing or lamination. The white chalk is faintly laminated. The color of the ooze grades into olive yellow (2.5Y6/6) marl in the CC.
BARREMIAN	IAPTIAN	C 13 (blow Zone) F/PR/MF/PR/P					42 % 6 % 69 %	2	CC				* * * *	SMEAR SLIDE SUMMARY (%):  1,77 2,37 2,44 2,55 CC,27 CC D M D D M D  TEXTURE:  Silt — — — — 2 — Clay 100 100 100 100 98 100  COMPOSITION:  Quartz Tr — Tr — Tr — Feldspar — — — — Tr — Mica Tr — Tr — Tr — Clay 89 99 85 <10 87 — Calcite/Dolomite 5 Tr 15 60 — 85 Accessory Minerals 5 — Tr Tr Tr — Fe/Mn Oxide — 1 — — — — Foraminifers — Tr — Tr — — Nannofossils — — — 30 10 15  PHYSICAL PROPERTIES DATA:  1,50 1,101 CC,19 CC,20  V <sub>p</sub> (c) — 1.70 1.65 — ρ <sub>b</sub> — 1.87 1.88 — T <sub>c</sub> 2.61 — — 2.80





SITE 640 HOLE A CORE 3 R CORED INTERVAL 5355.2-5364.8 mbsl; 164.7-174.3 mbsf

TIME-ROCK UNIT	BIOSTRAT. ZONE/ FOSSIL CHARACTER				PALEOMAGNETICS	PHYS. PROPERTIES	CHEMISTRY	SECTION	METERS	GRAPHIC LITHOLOGY	DRILLING DISTURB.	SED. STRUCTURES	SAMPLES	LITHOLOGIC DESCRIPTION
	FORAMINIFERS	NANNOFOSSILS	RADIOLARIANS	DIATOMS										
LATE BARREMIAN	B	CC-6	A/G		■	■	88 %	1	0.5 1.0				* * * * *	GRAY MARL/CLAY TURBIDITES and WHITE CLAYEY OOZE.  The top 3 cm of the core is nanno chalk. This is underlain by dark gray (5Y5/1) calcareous clay and marl, and white (5G7/1 and 5G 8/1), clayey ooze to chalk. The marl and clayey ooze alternate at intervals of 50 to 100 cm. In some cases the dark gray marl layers have sharp bases and gradational tops; in others both upper and lower boundaries are gradational. The beds are finely, though faintly, laminated and contain abundant plant debris, including some wood fragments. They thus represent increased terrigenous input both as distal turbidites and by nepheloid transport. The clayey ooze layers (pelagic intervals) are massive and faintly mottled. They consist largely of recrystallized carbonate with some nanno-fossils including nannoconids. Some beds contain intervals which are darker in color and more clay-rich. The chalk has been lithified to gray clayey limestone at Section 1, 110-120 cm and 146-148 cm, and a limestone pebble occurs at the bottom of Section 4.
	A/M	A/M	A/M		■	■	88 %	2					* * * * *	
	A/M	A/M	A/M		■	■	88 %	3					* * * * *	
	A/M	A/M	A/M		■	■	88 %	4					* * * * *	
	A/M	A/M	A/M		■	■	88 %	5					* * * * *	

## GRAY MARL/CLAY TURBIDITES and WHITE CLAYEY OOZE.

The top 3 cm of the core is nanno chalk. This is underlain by dark gray (5Y5/1) calcareous clay and marl, and white (5G7/1 and 5G 8/1), clayey ooze to chalk. The marl and clayey ooze alternate at intervals of 50 to 100 cm. In some cases the dark gray marl layers have sharp bases and gradational tops; in others both upper and lower boundaries are gradational. The beds are finely, though faintly, laminated and contain abundant plant debris, including some wood fragments. They thus represent increased terrigenous input both as distal turbidites and by nepheloid transport. The clayey ooze layers (pelagic intervals) are massive and faintly mottled. They consist largely of recrystallized carbonate with some nanno-fossils including nannoconids. Some beds contain intervals which are darker in color and more clay-rich. The chalk has been lithified to gray clayey limestone at Section 1, 110-120 cm and 146-148 cm, and a limestone pebble occurs at the bottom of Section 4.

## SMEAR SLIDE SUMMARY (%):

1,116	1,137	2,88	2,125	3,133	4,10
D	D	D	D	D	D

## TEXTURE:

Silt	10	20	—	—	—	—
Clay	90	80	100	100	100	0

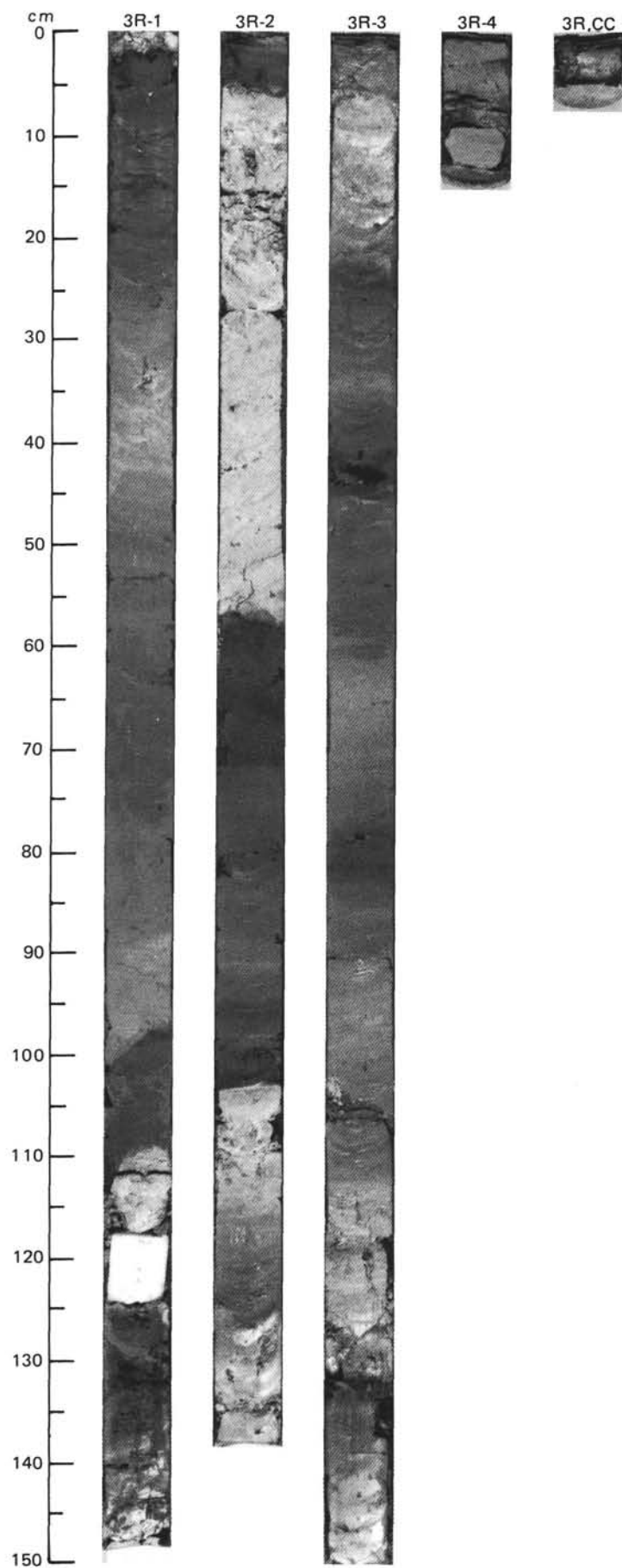
## COMPOSITION:

Quartz and Feldspar	—	1	—	—	—	Tr
Mica	—	1	—	—	—	—
Clay	—	40	75	40	65	15
Calcite/Dolomite	90	—	—	—	Tr	—
Accessory Minerals	—	—	—	—	10	—
Pyrite	—	5	Tr	Tr	—	—
Nannofossils	10	50	25	60	25	5
Radiolarians	—	—	—	Tr	—	20*
Sponge Spicules	—	—	Tr	—	—	—
Fish Remains	—	—	—	—	—	Tr
Plant Debris	—	5	—	—	—	—
Micrite	—	—	—	—	—	60

\*Calcite replaced.

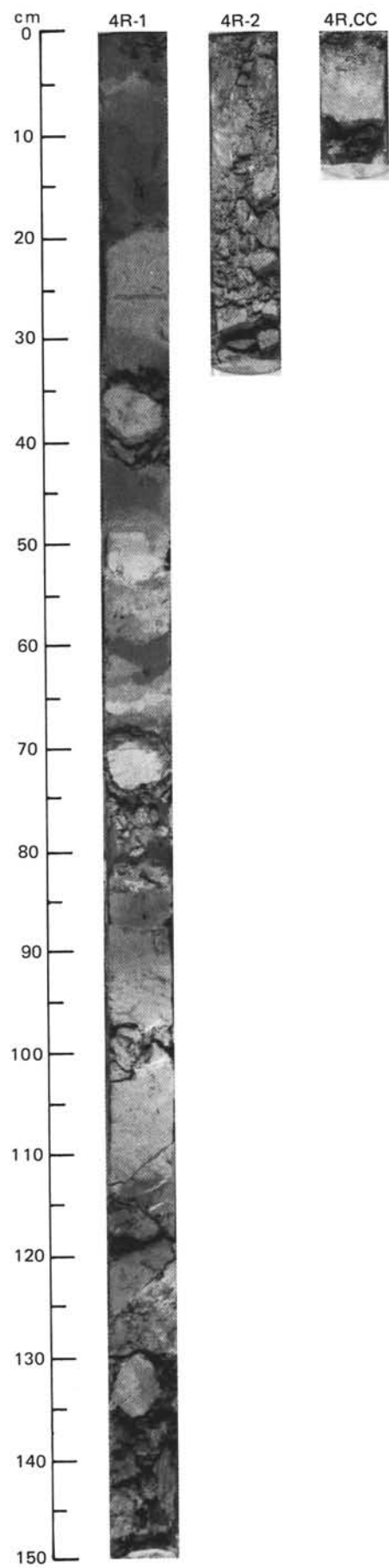
## PHYSICAL PROPERTIES DATA:

	1.50	1,141	2,139	3,50	3,141	4,13
V <sub>p</sub> (a)	—	1.48	1.75	—	1.66	3.31
ρ <sub>b</sub>	—	1.76	1.92	—	1.86	2.28
T <sub>c</sub>	2.84	—	—	2.55	—	—



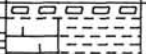
SITE 640 HOLE A CORE 4 R CORED INTERVAL 5364.8-5374.5 mbsl; 174.3-184.0 mbsf

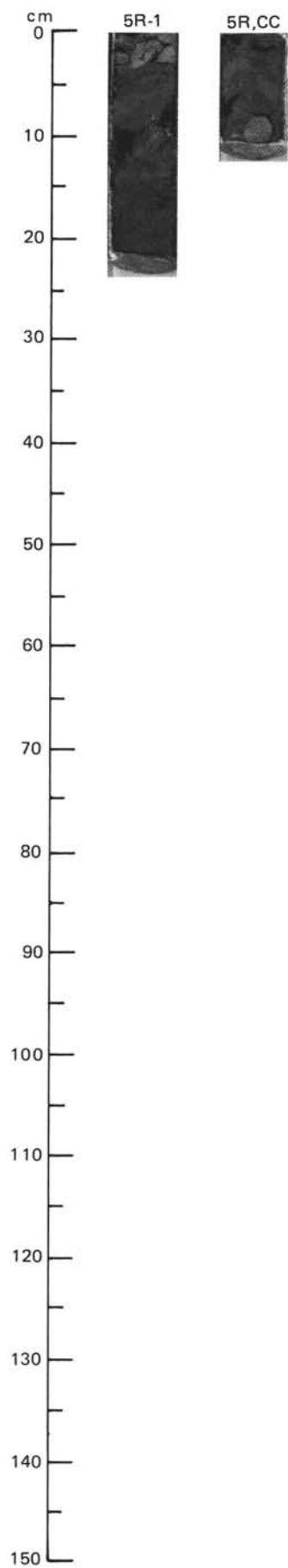
TIME-ROCK UNIT	BIOSTRAT. ZONE/ FOSSIL CHARACTER				PALEOMAGNETICS	PHYS. PROPERTIES	CHEMISTRY	SECTION	METERS	GRAPHIC LITHOLOGY	DRILLING DISTURB.	SED. STRUCTURES	SAMPLES	LITHOLOGIC DESCRIPTION
	FORAMINIFERS	NANNOFOSSILS	RADIOLARIANS	DIATOMS										
LATE HAUTERIVIAN / EARLY BARREMIAN	R/P	C/M	C/M	B	■	65 % ●	1	0.5 1.0				**	GRAY MARL (STONE) and LIMESTONE.  The core consists of light gray (5Y8/1), medium gray (5Y7/1) and dark gray (5Y5/1) firm marl or marlstone, apparently interbedded, though all the contacts are probably drilling contacts. Clayey limestones occur in Section 1 at 34-42 cm, 70-80 cm, and 130-137 cm. A piece of wood 1.5 x 0.5 x 5 cm was found in Section 1 at 120 cm.	
					■	63 % ●	2 CC					*	SMEAR SLIDE SUMMARY (%):  1,12 1,23 2,14 D D D  TEXTURE:  Silt 10 — — Clay 90 100 100  COMPOSITION:  Quartz — Tr — Clay 50 40 32 Calcite/Dolomite — 25 35 Accessory Minerals Tr Tr 3 Nannofossils 40 30 30 Sponge Spicules < 2 — — Plant Debris 5 5 —  PHYSICAL PROPERTIES DATA:  1,16 1,70 CC,6  Vρ (a) — — 1.85 ρb 1.79 — 2.01 Tc — 3.04 —	





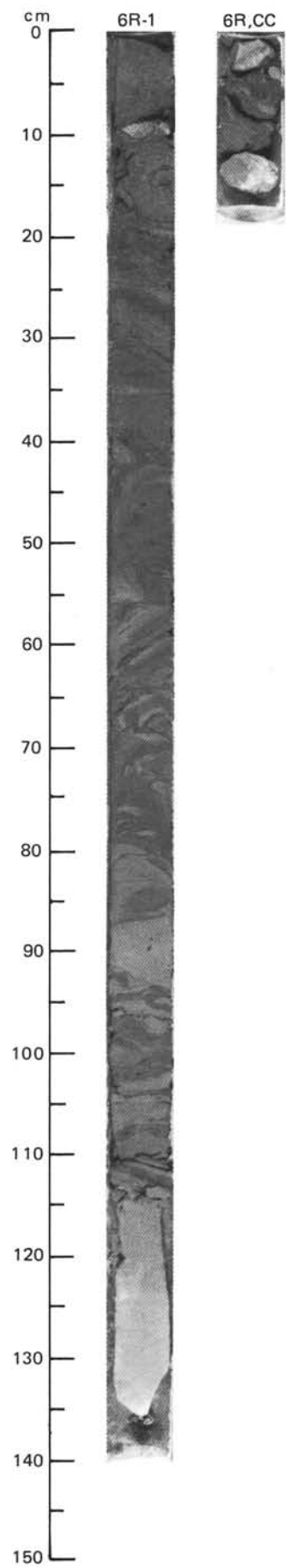
SITE 640 HOLE A CORE 5 R CORED INTERVAL 5374.5-5384.2 mbsl; 184.0-193.7 mbsf

TIME-ROCK UNIT	BIOSTRAT. ZONE/ FOSSIL CHARACTER				PALEOMAGNETICS	PHYS. PROPERTIES	CHEMISTRY	SECTION	METERS	GRAPHIC LITHOLOGY	DRILLING DISTURB.	SED. STRUCTURES	SAMPLES	LITHOLOGIC DESCRIPTION
	FORAMINIFERS	NANNOFOSSILS	RADIOLARIANS	DIATOMS										
HAUTERIVIAN	R/M	C/G	F/P			■	36 % ●	1					*	<p><b>NANNOFOSSIL CHALK and MARLSTONE.</b></p> <p>The core consists of medium gray (5Y6/1) nannofossil chalk and dark gray (5Y4/1) marlstone.</p> <p><b>SMEAR SLIDE SUMMARY (%):</b></p> <p style="text-align: right;">1,18 D</p> <p><b>TEXTURE:</b></p> <p>Silt 5 Clay 95</p> <p><b>COMPOSITION:</b></p> <p>Clay 48 Calcite/Dolomite Tr Accessory Minerals 1 Nannofossils 45 Plant Debris 5</p> <p><b>PHYSICAL PROPERTIES DATA:</b></p> <p style="text-align: right;">CC,5</p> <p><math>V_p</math> (a) 1.60 <math>\rho_b</math> 1.82</p>
		<i>Cretarhabdus loriei</i> Zone (CC-4 b)												



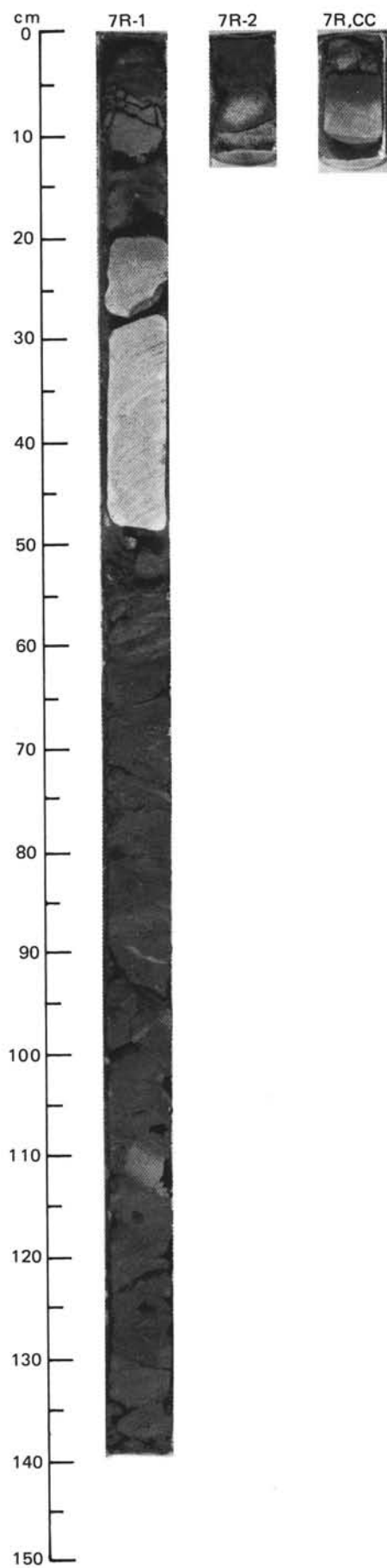
SITE 640 HOLE A CORE 6 R CORED INTERVAL 5384.2-5393.8 mbsl; 193.7-203.3 mbsf

TIME-ROCK UNIT	BIOSTRAT. ZONE/ FOSSIL CHARACTER				PALEOMAGNETICS	PHYS. PROPERTIES	CHEMISTRY	SECTION	METERS	GRAPHIC LITHOLOGY	DRILLING DISTURB.	SED. STRUCTURES	SAMPLES	LITHOLOGIC DESCRIPTION																																																																																
	FORAMINIFERS	NANNOFOSSILS	RADIOLARIANS	DIATOMS																																																																																										
HAUTERIVIAN	R/P	C/M	CC-4 b			■	● 13 %	1	0.5		/	/	*	SILTY CLAY MICROTURBIDITES and LIMESTONE.																																																																																
						■	● 89 %		1.0																																																																																					
								CC																																																																																						
<p>The core consists of interbedded calcareous clay and silty calcareous clay. Interbedding is on the scale of 0.1 to 3 cm. Each bed is normally graded from dark gray (5Y4/1) silty calcareous clay, rich in mica and plant debris, up into lighter gray (5Y5/1) calcareous clay. The lower part of each interval commonly shows parallel lamination. Several thin ( 1 cm) marl interbeds occur. The whole section is badly fractured and disturbed either by drilling or by natural slumping.</p> <p>Light gray, structureless clayey limestone occurs at the bottom of Section 1 and in the CC.</p> <p>SMEAR SLIDE SUMMARY (%):</p> <table><tr><td></td><td>1,48</td><td>1,93</td><td>1,136</td></tr><tr><td></td><td>D</td><td>M</td><td>D</td></tr></table> <p>TEXTURE:</p> <table><tr><td>Silt</td><td>11</td><td>—</td><td>—</td></tr><tr><td>Clay</td><td>89</td><td>100</td><td>—</td></tr></table> <p>COMPOSITION:</p> <table><tr><td>Quartz</td><td>11</td><td>—</td><td>1</td></tr><tr><td>Mica</td><td>—</td><td>Tr</td><td>—</td></tr><tr><td>Clay</td><td>60</td><td>73</td><td>—</td></tr><tr><td>Calcite/Dolomite</td><td>Tr</td><td>7</td><td>—</td></tr><tr><td>Accessory Minerals</td><td>Tr</td><td>Tr</td><td>—</td></tr><tr><td>Nannofossils</td><td>25</td><td>20</td><td>—</td></tr><tr><td>Fish Remains</td><td>—</td><td>Tr</td><td>—</td></tr><tr><td>Plant Debris</td><td>4</td><td>—</td><td>—</td></tr><tr><td>Microspar</td><td>—</td><td>—</td><td>89</td></tr><tr><td>Micrite</td><td>—</td><td>—</td><td>10</td></tr></table> <p>PHYSICAL PROPERTIES DATA:</p> <table><tr><td></td><td>1,49</td><td>1,60</td><td>1,132</td></tr><tr><td>V<sub>p</sub> (a)</td><td>1.69</td><td>—</td><td>3.48</td></tr><tr><td>V<sub>p</sub> (b)</td><td>—</td><td>—</td><td>3.55</td></tr><tr><td>V<sub>p</sub> (c)</td><td>—</td><td>—</td><td>3.55</td></tr><tr><td>ρ<sub>b</sub></td><td>1.89</td><td>—</td><td>2.49</td></tr><tr><td>T<sub>c</sub></td><td>—</td><td>3.16</td><td>—</td></tr></table>																1,48	1,93	1,136		D	M	D	Silt	11	—	—	Clay	89	100	—	Quartz	11	—	1	Mica	—	Tr	—	Clay	60	73	—	Calcite/Dolomite	Tr	7	—	Accessory Minerals	Tr	Tr	—	Nannofossils	25	20	—	Fish Remains	—	Tr	—	Plant Debris	4	—	—	Microspar	—	—	89	Micrite	—	—	10		1,49	1,60	1,132	V <sub>p</sub> (a)	1.69	—	3.48	V <sub>p</sub> (b)	—	—	3.55	V <sub>p</sub> (c)	—	—	3.55	ρ <sub>b</sub>	1.89	—	2.49	T <sub>c</sub>	—	3.16	—
	1,48	1,93	1,136																																																																																											
	D	M	D																																																																																											
Silt	11	—	—																																																																																											
Clay	89	100	—																																																																																											
Quartz	11	—	1																																																																																											
Mica	—	Tr	—																																																																																											
Clay	60	73	—																																																																																											
Calcite/Dolomite	Tr	7	—																																																																																											
Accessory Minerals	Tr	Tr	—																																																																																											
Nannofossils	25	20	—																																																																																											
Fish Remains	—	Tr	—																																																																																											
Plant Debris	4	—	—																																																																																											
Microspar	—	—	89																																																																																											
Micrite	—	—	10																																																																																											
	1,49	1,60	1,132																																																																																											
V <sub>p</sub> (a)	1.69	—	3.48																																																																																											
V <sub>p</sub> (b)	—	—	3.55																																																																																											
V <sub>p</sub> (c)	—	—	3.55																																																																																											
ρ <sub>b</sub>	1.89	—	2.49																																																																																											
T <sub>c</sub>	—	3.16	—																																																																																											

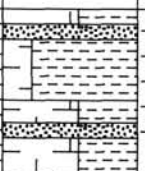




566








SITE 640 HOLE A CORE 8 R CORED INTERVAL 5403.5-5413.0 mbsl; 213.0-222.5 mbsf

TIME-ROCK UNIT	BIOSTRAT. ZONE/ FOSSIL CHARACTER				PALEOMAGNETICS	PHYS. PROPERTIES	CHEMISTRY	SECTION	METERS	GRAPHIC LITHOLOGY	DRILLING DISTURB.	SED. STRUCTURES	SAMPLES	LITHOLOGIC DESCRIPTION											
	FORAMINIFERS	NANNOFOSSILS	RADIOLARIANS	DIATOMS																					
HAUTERIVIAN	R/P	C/M CC-4b	B			■ ■ ● 23 %	1	0.5					<p><b>SANDY TURBIDITES.</b></p> <p>The core consists of three interbedded lithologies: (1) gray (5Y6/1) marlstone; (2) dark gray (5Y3/1) calcareous claystone; (3) dark gray (5Y5/1) fine silt- to fine sandstone. The fine sandstones show faint lamination and normally graded bedding (Tb, Td-e).</p> <p>Pyrite nodules occur in several places, e.g. Section 1, 0-2 cm.</p> <p><b>PHYSICAL PROPERTIES DATA:</b></p> <table><tr><td></td><td>1,39</td><td>1,43</td></tr><tr><td><math>V_p</math> (a)</td><td>1.80</td><td>—</td></tr><tr><td><math>\rho_b</math></td><td>2.01</td><td>—</td></tr><tr><td><math>T_c</math></td><td>—</td><td>3.92</td></tr></table>		1,39	1,43	$V_p$ (a)	1.80	—	$\rho_b$	2.01	—	$T_c$	—	3.92
	1,39	1,43																							
$V_p$ (a)	1.80	—																							
$\rho_b$	2.01	—																							
$T_c$	—	3.92																							

SITE 640 HOLE A CORE 9 R CORED INTERVAL 5413.0-5422.7 mbsl; 222.5-232.2 mbsf

TIME-ROCK UNIT	BIOSTRAT. ZONE/ FOSSIL CHARACTER				PALEOMAGNETICS	PHYS. PROPERTIES	CHEMISTRY	SECTION	METERS	GRAPHIC LITHOLOGY	DRILLING DISTURB.	SED. STRUCTURES	SAMPLES	LITHOLOGIC DESCRIPTION
	FORAMINIFERS	NANNOFOSSILS	RADIOLARIANS	DIATOMS										
HAUTERIVIAN	CC-4 b	F/M												<p><b>LIMESTONE and SANDSTONE.</b></p> <p>The core consists of a fragment of light gray (2.5Y7/0) clayey limestone overlying three pieces of coarse gray (N4, N5) sandstone, faintly laminated and graded from very coarse to fine sand size.</p> <p><b>THIN SECTION SUMMARY (%):</b></p> <p>1,18-20 D</p> <p><b>TEXTURE:</b></p> <p>Sand 98 Silt 2</p> <p><b>COMPOSITION:</b></p> <p>Quartz 30 Feldspar 17 Calcite 45 Foraminifers Tr Bioclasts 1 Oncolites 1 Micrite Lithoclasts 1</p>

